

Seismic hazard maps and spectrum for Patna considering region-specific seismotectonic parameters

P. Anbazhagan¹ · Ketan Bajaj¹ · Satyajit Patel²

Received: 28 April 2014 / Accepted: 13 April 2015 / Published online: 24 April 2015
© Springer Science+Business Media Dordrecht 2015

Abstract The objective of this paper was to develop the seismic hazard maps of Patna district considering the region-specific maximum magnitude and ground motion prediction equation (GMPEs) by worst-case deterministic and classical probabilistic approaches. Patna, located near Himalayan active seismic region has been subjected to destructive earthquakes such as 1803 and 1934 Bihar–Nepal earthquakes. Based on the past seismicity and earthquake damage distribution, linear sources and seismic events have been considered at radius of about 500 km around Patna district center. Maximum magnitude (M_{\max}) has been estimated based on the conventional approaches such as maximum observed magnitude (M_{\max}^{obs}) and/or increment of 0.5, Kijko method and regional rupture characteristics. Maximum of these three is taken as maximum probable magnitude for each source. Twenty-seven ground motion prediction equations (GMPEs) are found applicable for Patna region. Of these, suitable region-specific GMPEs are selected by performing the ‘efficacy test,’ which makes use of log-likelihood. Maximum magnitude and selected GMPEs are used to estimate PGA and spectral acceleration at 0.2 and 1 s and mapped for worst-case deterministic approach and 2 and 10 % period of exceedance in 50 years. Furthermore, seismic hazard results are used to develop the deaggregation plot to quantify the contribution of seismic sources in terms of magnitude and distance. In this study, normalized site-specific design spectrum has been developed by dividing the hazard map into four zones based on the peak ground acceleration values. This site-specific response spectrum has been compared with recent Sikkim 2011 earthquake and Indian seismic code IS1893.

Electronic supplementary material The online version of this article (doi:[10.1007/s11069-015-1764-0](https://doi.org/10.1007/s11069-015-1764-0)) contains supplementary material, which is available to authorized users.

✉ P. Anbazhagan
anbazhagan@civil.iisc.ernet.in

¹ Department of Civil Engineering, Indian Institute of Science, Bangalore, India

² Applied Mechanics Department, S.V. National Institute of Technology, Surat, India

Keywords Earthquake · Hazards · Maximum magnitude · GMPE · PGA · SA

1 Introduction

Earthquake has played a devastating role in terms of human casualties and infrastructural damages. Its unpredictable nature can cause multiple hazards such as ground motion, ground shaking, site effects, ground displacement, fire, liquefaction, landslide and Tsunami. In India, urban centers and cities are more susceptible to earthquake hazards due to high population density, improper planning, poor land use and substandard construction practices. Many great events including 1905 Kangra, 1934 Bihar–Nepal, 1960 Chilean, 1985 Mexico, 1989 Loma Prieta, 2004 Sumatra and 2011 Sendai earthquakes have originated from subduction zone. Subduction zones having a seismic gap make the scenario worse, and high-frequency and large-magnitude earthquakes originate from these zones. Various researchers have highlighted that the Central Seismic Gap in Himalayan region is one of the most seismically active regions in the world (Khattri 1987), which may be the source of great events in the future. Even though many enhancements have been made in earthquake resistant design of structures, still it requires more systematic understanding and construction practice to minimize loss of lives and damages in developing countries. Due to rapid development, population growth and increase in seismicity in India, there is a demand for the estimation of region-specific seismic hazard parameters such as site classification, amplification, site effects, liquefaction and landslide for the seismic microzonation of cities near active Himalaya. During the last few decades, India has experienced several destructive earthquakes. About 60 % of the country is susceptible to damaging levels of seismic hazard (NDMA 2010). The first and foremost step toward reducing earthquake hazard is forecasting the same precisely on a regional scale. Determining the seismic hazard parameters such as peak ground acceleration and response spectra is important for infrastructure and building design and also for disaster planning and management. Such study is mandatory and needs to be carried out for cities close to or in the highly active seismic region of the world, where the occurrence of a large-magnitude earthquake is comparatively frequent such as an active region of India.

Seismic hazard estimation is a prime step in the seismic microzonation, where micro-level variations of seismic hazard and its effects are quantified and mapped. In this study, the seismic hazard of Patna district has been estimated considering region-specific parameters such as seismic study area, maximum magnitude and suitable attenuation relations. The seismic study area has been selected considering past damage distribution, i.e., isoseismal map. Maximum magnitude from each linear source has been estimated using conventional methods of increment of 0.5 in maximum observed magnitude ($M_{\text{obs}}^{\text{max}}$) based on 'b' values, Kijko method (Kijko and Sellevoll 1989) and regional rupture characteristics (Anbazhagan et al. 2014, 2015). The maximum of all these methods has been assigned to each source. Further best-suited ground motion prediction equation (GMPE) for a region has been selected from the twenty-seven applicable GMPEs for Patna seismic study area (SSA). Segmented GMPE ranking has been followed to select GMPEs by carrying out 'efficacy test,' which makes use of log-likelihood (LLH) given by Scherbaum et al. (2009) and Delavaud et al. (2009). The seismic hazard maps have been generated by considering the worst-case deterministic scenario and classical probabilistic approaches. Probabilistic seismic hazard analysis (PSHA) values are estimated for 2 and 10 % probability of

exceedance for 50 years, i.e., for the return period of 2475 and 475 years. Furthermore, the computed hazard in terms of spectral acceleration at 0.2 and 1 s is mapped, and deaggregation plot has been developed to understand the hazard contribution from various combinations of magnitude and hypocentral distance. In addition to that, site-specific normalized design spectrum has been developed by deterministic approach and PSHA for 2 and 10 % probability of exceedance in 50 years and compared with Sikkim 2011 earthquake and Indian Standard IS-1893 (2002).

2 Study area

Patna, the capital of Bihar, is one of the oldest continuously inhabited places in the world. Ancient Patna, known as Pataliputra, was the capital of the Magadha Empire under Har-yanka, Nanda, Mauryan, Sunga, Gupta and Pala. The Patna district center point having latitude 25.611°N and longitude 85.144°E is situated on the southern bank of the Ganges. The city also straddles the rivers Sone, Gandak and Punpun. The study area of Patna belongs to the Seismic zone IV in current Seismic Zonation map of India (IS: 1893 2002), with zone factor of 0.24.

Various researchers have taken different radii of consideration around the city center to generate a seismotectonic map of the study area. Anbazhagan et al. (2013b) recommended that a seismic study area (SSA) radius should be decided by taking into account seismicity of the region and past damage distribution. In this study, isoseismal map, i.e., damage distribution map and location of Main Boundary Thrust, Main Central Thrust and Himalayan Frontal Thrust (HFT) has been considered to select SSA. Structural damage of European Macroseismic (EMS) intensity V and above has been reported beyond 350 km during Bihar–Nepal earthquake (1934) of moment magnitude (M_w) 8.0 with epicenter at 26.6°N and 86.80°E (Nath et al. 2009). Also, 1833 Nepal earthquake of 7.6 M_w which damaged the Indo-Gangetic basin (IGB) for more than 450 km was reported (Ambraseys and Douglas 2004). These two intensity maps are shown in Fig. 1a, b, respectively. Based on this information, it can be inferred that any earthquake occurring up to 500 km radius around Patna may cause damage to Patna city. So, the radius of SSA has been selected as 500 km, and seismotectonic parameters were collected and discussed in the next section. Figure 2 shows the study area of Patna with Himalayan belt and IGB.

3 Seismotectonics of Patna

In order to perform seismic hazard analysis, information about seismic feature such as faults, shear zones and lineaments with all earthquake events occurred in the SSA is mandatory (Anbazhagan et al. 2013b). In this study, seismic features observed around 500 km radius of Patna have been collected. SSA covers most part of the IGB, which extends between 24°30'N latitude to 77°88' E longitude and covers an area of approximately 250,000 km². It is identified as one of the most densely populated regions of India, and around 200 million people reside in the basin (Kumar et al. 2013). The formation of IGB is a consequence of collision between Eurasian and Indian plate, which has caused the rise of Himalayas since Cenozoic era. The Ganga is the main river of the basin, which is formed owing to the upliftment of Himalaya after the collision of Indian and Asian Plates (Dewey and Bird 1970). The Ganga River flows from the Himalayas in the

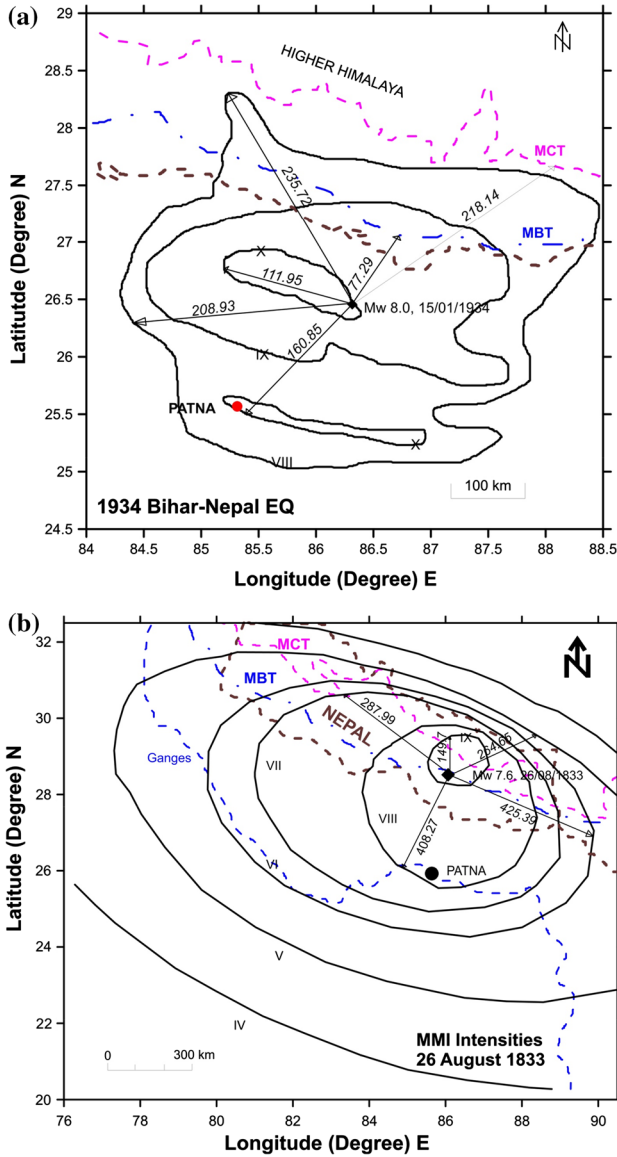


Fig. 1 **a** Damage distribution map of 1934 Bihar–Nepal earthquake (modified after Kayal 2008), **b** damage distribution map of 1833 Bihar–Nepal earthquake (modified after Ambraseys and Douglas 2004)

north to the Bay of Bengal in the north-west. The weathering by river Ganga during its course of flow results in deposition of sediments in the lower course. The significant amount of deposition of these sediments in the Indo-Gangetic basin over a long period resulted in thick fluvial deposit. This deposit consists of different layers of sediments with an overall thickness of up to several kilometers in many parts of IGB (Sinha et al. 2005; Anbazhagan et al. 2012; Kumar et al. 2013). Many important cities such as Patna, Meerut, Lucknow, Kanpur, Aligarh, Gorakhpur, Agra and Jhansi located in different parts of the

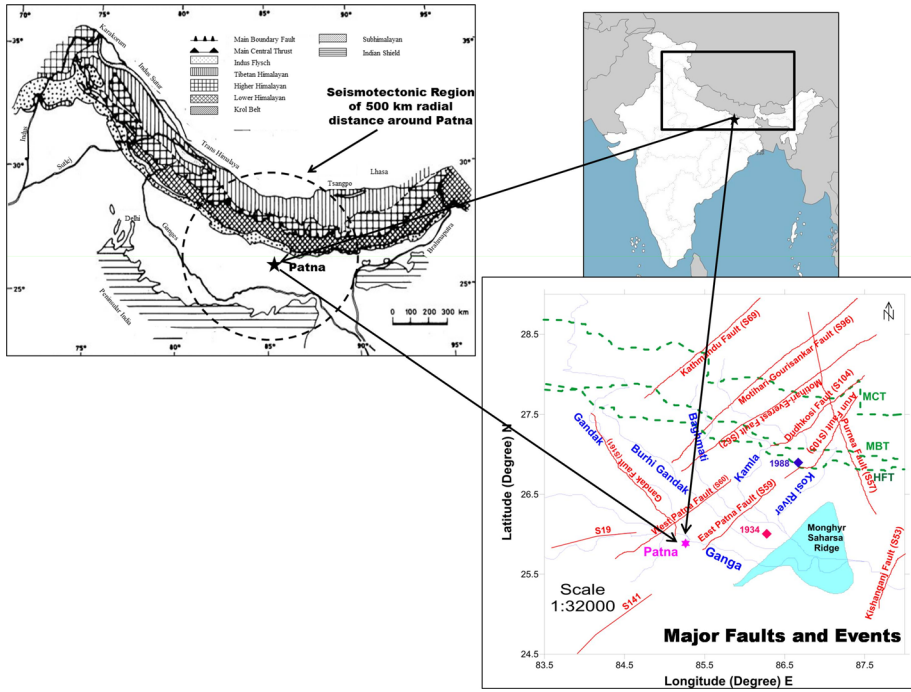


Fig. 2 Study area of Patna along with river system and structural feature based on Dasgupta et al. (1987), Dasgupta et al. (1993) and GSI (2000). *MCT* Main Central Thrust, *MBT* Main Boundary Thrust, *HFT* Himalayan Frontal Thrust (modified after Gansser 1964)

IGB are susceptible to earthquake damages due to the proximity to seismically active Himalayan belt and situated on thick soil deposits. Also, IGB consists of many active tectonic features such as Munger–Saharsa Ridge Fault, Monghyr–Saharsa Ridge Fault, East Patna Fault, West Patna Fault, Delhi–Haridwar Ridge, Delhi–Muzaffarabad Ridge and Faridabad Ridge. The major earthquakes such as 1833 Bihar, 1934 Bihar–Nepal, 1988 Bihar–Nepal and 2011 Delhi Earthquakes have occurred in IGB. The study area is surrounded by several active faults and covered with thick soil deposits as shown in Fig. 2. Regional seismic records designate that deep regions of North Bihar Plains (area between 24.33°E–27.52°E latitude and 82.33°N–88.29°N longitude) are tectonically active. This part has documented more than 100 seismic events with 46 events of magnitude larger than 4.5 through the period of 1934–1993 (GSI 2000). In the northeast Patna region, the key faults are West and East Patna Faults in the East Ganga basin (See Fig. 2). These faults are acknowledged as transverse faults, and the occurrence of seismic events is due to stimulus of fluvial dynamics in the North Patna plains transverse faults (Valdiya 1976; Dasgupta et al. 1987). The East Patna Fault (EPF) is considered to be the most active fault, and its interaction with Himalayan Frontal Thrust is characterized by a cluster of earthquakes (Banghar 1991; GSI 2000). This fault is located in the part of the city area. The Gandak River in the western basin of the Baghmata river basin is flowing along the Gandak Fault (Mohindra et al. 1992), which is also located near Patna district center (see Fig. 2). Dasgupta et al. (1993) ventured that all other faults between Motihari and Kishanganj have the same possibility of seismic hazard as they form a part of related fault system. The study

area Patna is near the above-mentioned fault. Till date, the state of Bihar has faced a number of earthquakes, which include devastating earthquakes like 1934 Bihar–Nepal Earthquake, having a magnitude of 8.0, which killed nearly 10,700 people. Many earthquakes have also occurred during 1833, at Bihar–Nepal border. Various earthquakes like 1927 Madhya Pradesh earthquake, 1985 Rajauli area earthquake and 1988 Udaypur Gary earthquake have affected Patna in terms of the financial loss and loss of lives. Apart from the local seismic activity around Patna, the area also located within a radial distance of approximately 250 km from Main Boundary Thrust (MBT) and the Main Central Thrust (MCT), where many major earthquakes have been reported and are also considered. Considering the above seismic aspects of areas in and around Patna, Patna district center can be considered under a high seismic risk.

4 Seismicity around Patna

Seismicity of the study area is a basic and indispensable concern to be scrutinized in seismic hazard analysis for assessing seismic risk. The tectonic feature of the study area has been collected from the Seismotectonic Atlas (SEISAT) published by the Geological survey of India (GSI) (SEISAT 2000). The well-defined and acknowledged seismic source has been compiled in published seismotectonic maps as hard copy in 2000 and updated soft copy in 2010. It contains forty-three maps in 42 sheets of $3^\circ \times 4^\circ$ size with a scale of 1:10,00,000. As part of the present study for the preparation of seismotectonic map, linear sources are taken from SEISAT and verified with seismotectonic map prepared by Kolathayar et al. (2012) for whole India and Kumar et al. (2013) for Lucknow region. These maps were scanned using a high-resolution scanner and digitized for identification of the linear sources in 500 km radius from Patna city center. No aerial source has been considered in this study as proper distribution of linear source is available. Demarcation of MBT and MCT has been done in the seismotectonic map, and all the faults have also been named.

The earthquake event details within 500 km radius around the Patna district compiled from several resources like National Earthquake Information Centre (NEIC), International Seismological Centre, Indian Meteorological Department (IMD), United State Geological Survey (USGS), Northern California Earthquake Data Centre (NCEDC) and Geological Survey of India have been used. A total of 2326 events have been collected, which consist of epicenter coordinates, year, month, date, focal depth and magnitude in different magnitude scale. The collected data were reported in different magnitude scale as body magnitude (m_b), Richter or local magnitude (M_L), surface wave magnitude (M_S) and moment magnitude (M_w). In order to attain consistency and homogeneity, all the reported events were converted into M_w , which is more reliable. The numerous empirical relationships were developed between these magnitudes by various researchers (Stromeyer et al. 2004; Castellaro et al. 2006; Scordilis 2006; Bormann et al. 2007; Thingbaijam et al. 2008; Sreevalsa et al. 2011). Scordilis (2006) relation has been used in the present study, which includes worldwide data.

In order to filter the main event from the dependent event (i.e., clusters, foreshocks and aftershocks), declustering of earthquake catalogue is required. For achieving the best result of hazard analysis (Wiemer and Wyss 1994; 1997) and for seismicity rate study (Frankel 1995), declustering of earthquake catalogue is necessary. As far as the phenomenon of the Poisson model of earthquake occurrence is concerned, i.e., the earthquake took place

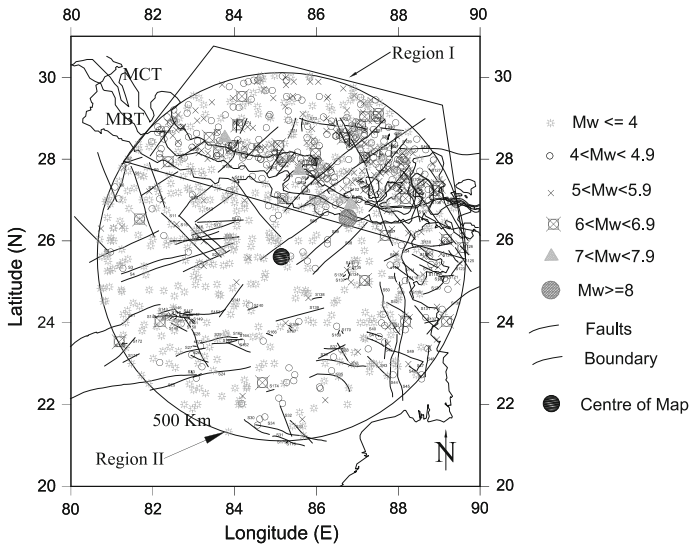


Fig. 3 Seismotectonic map of Patna

randomly, a seismicity model needs to be declustered. For the removal of dependent events such as aftershocks and before shocks, several methods were suggested (Savage 1972; Gardner and Knopoff, 1974; Reasenber 1985; Davis and Frohlich 1991; Molchan and Dmitrieva 1992). In the present study, algorithms developed by Gardner and Knopoff (1974) and modified by Uhrhammer (1986) are used. As per Stiphout et al. (2010), seismicity derived by a static window method (Reasenber 1985) does not go behind Poisson distribution. Out of 2325 events, 54 % were found to be depended events; a total 1262 events have been acknowledged as main shock. For further analysis, $M_w \geq 4$ (i.e., 818 events) were considered, as smaller magnitude would not generate considerable ground motions for building damage. The complete catalogue contains 444 events with M_w less than 4. In order to develop seismotectonic map, declustered earthquake events are superimposed with the source map as shown in Fig. 3. It has been seen from Fig. 3 that events are more densely located near MBT and MCT as compared to other areas. The study area is divided into two regions, i.e., Region I (belonging to MBT and MCT) and Region II, depending upon the events allocation. List of numbers of earthquake events with M_w equal to or greater than 4 is given in Table 1 for both Regions I and II. These regions are divided using trapezoid as shown in Fig. 3, Region I belongs to events inside the trapezoid, and Region II belongs to events outside the trapezoid. Both the regions are evaluated separately for the seismic hazard estimation.

5 Data completeness and G–R recurrence relationship

Assessments of the seismic parameters are the basic requirement in the determination of the seismic hazard map of a region. In order to predict the ground motion due to forthcoming earthquakes, it is obligatory to estimate these parameters. These parameters include the ‘a’ and ‘b’ parameters of Gutenberg–Richter (G–R) recurrence relationship (Gutenberg and Richter 1956). The earthquake catalogue presents the feature of seismicity

Table 1 Summary of earthquake events having M_w greater than or equal to 4

S. No.	Earthquake magnitude (M_w) range	Number of events	
		Region I	Region II
1.	$4 \leq M_w < 4.5$	66	39
2.	$4.5 \leq M_w < 5$	214	129
3.	$5 \leq M_w < 5.5$	140	88
4.	$5.5 \leq M_w < 6$	57	33
5.	$6 \leq M_w < 6.5$	18	16
6.	$6.5 \leq M_w < 7$	8	5
7.	$M_w \geq 7$	4	1

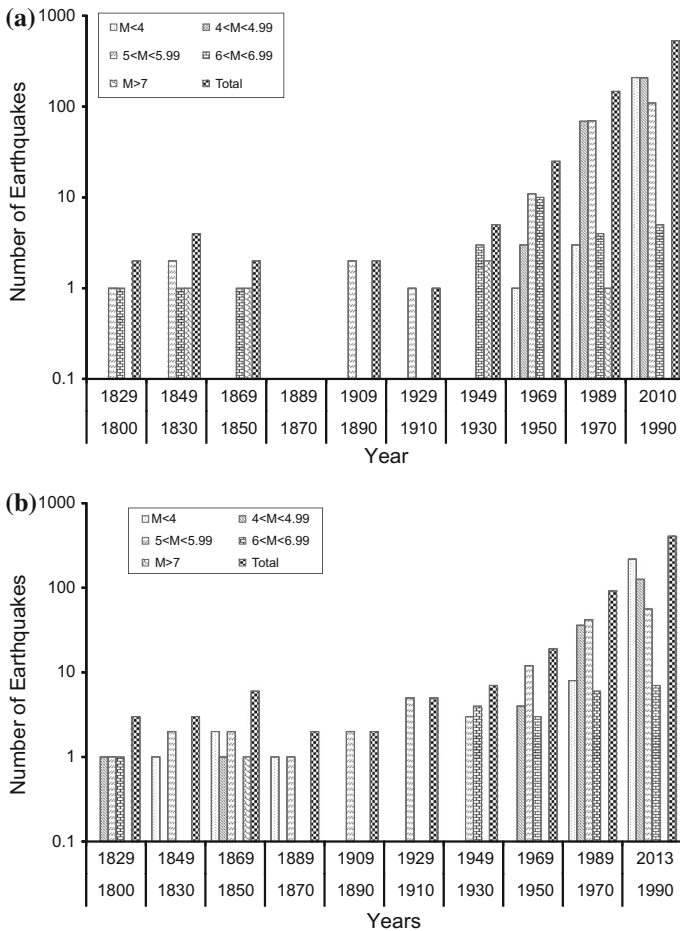


Fig. 4 **a** Histogram of earthquake data for Region I, **b** histogram of earthquake data for Region II

of a region, which is the backbone for seismic hazard analysis and involves in enlarging seismogenic zoning circumstances in combination with seismotectonic and geological information (Lai et al. 2009). To determine the seismicity characteristic of a region,

complete catalogue needs to be analyzed. Figure 4a, b shows the histogram of the Regions I and II, respectively, in SSA. Based on the observation from Fig. 4, one can predict that instrumented data for study area Patna might be recorded after Agra observatory laboratory shifted to Delhi and the number of observation increased to 15 in 1960 for Region II. As far as Region I is concerned, it has high instrumentally recorded seismic data after the seismology observatory started in Shimla with Omori Ewing seismograph in 1905. It can also be noted from these figures that no historic data are present with $M_w \leq 3$.

The seismicity parameters around the Patna site for Regions I and II can be quantified by the standard Gutenberg–Richter (G–R) recurrence relationship (Gutenberg and Richter 1956). It hypothesizes the existence of an exponential correlation between the mean annual rate of exceedance of an earthquake of specified magnitude and the magnitude for the period of completeness. The seismic recurrence rate can be assessed correctly if the collected data of the earthquake events are complete. Therefore, the composed data of Patna for the regions have to be scrutinized for its completeness. Stepp (1972) proposed a method to evaluate the duration of completeness of homogenized earthquake data by distributing it into small bins, seeing the variance of each bin as the same. The existence of earthquakes can be demonstrated as Poisson's distribution for the evaluation of effectual variance. Anbazhagan et al. (2010) has described the detailed procedure for completeness analysis as per Stepp (1972). The total compiled earthquake data in Region I cover a time period from 1816 to 2010 (or 194 years), while the data for Region II cover a time period from 1823 to 2013 (or 190 years). Both earthquake catalogues were examined independently to check the data completeness for each region. It has been comprehended that standard variation is found to be approximately parallel to $1/\sqrt{T}$ for the last 80 years for the earthquakes having moment magnitude less than 5.0 and for 110 years for higher magnitude. For Region II, the earthquake having moment magnitude less than 5.0 is complete for the last 70 years, whereas the higher magnitudes are complete for 110 years.

Maximum magnitude and its recurrence in the region depend on recurrence relation of regional seismicity data. This relation can also help to quantify uncertainty in the earthquake size of the region and/or every seismic source (Gutenberg and Richter 1956). The relation assumes exponential distribution of magnitude on every source and is also useful to estimate the minimum and maximum earthquake for any region. The recurrence law is defined by Gutenberg and Richter (1956) as given by the following equation

$$\log(N) = a - bM \quad (1)$$

where N resembles the number of earthquakes of magnitude M , ' a ' and ' b ' are positive real constants in which ' a ' denotes the seismic activity (log number of events with $M = 0$) and ' b ' describes the relative abundance of large to small shocks (Gutenberg and Richter 1956). After checking the completeness analysis of catalogue for both the regions, ' a ' and ' b ' parameters have been calculated. After determining the frequency of exceedance versus magnitude value, Gutenberg–Richter recurrence law for the zone can also be estimated. Figure 5 shows the G–R recurrence law for the Regions I and II with a correlation coefficient of 0.99 and 0.98, respectively. The ' b ' value for the Region I is 0.91 and for Region II is 1.01. These values are compared with that of the other researchers and shown in Table 2. This ' b ' value will be further used for the determination of maximum magnitude in the next section. The ' a ' value for Regions I and II for the present study is given as 5.32 and 4.98, respectively. These values are comparable with NDMA (2010) and Kumar et al. (2013).

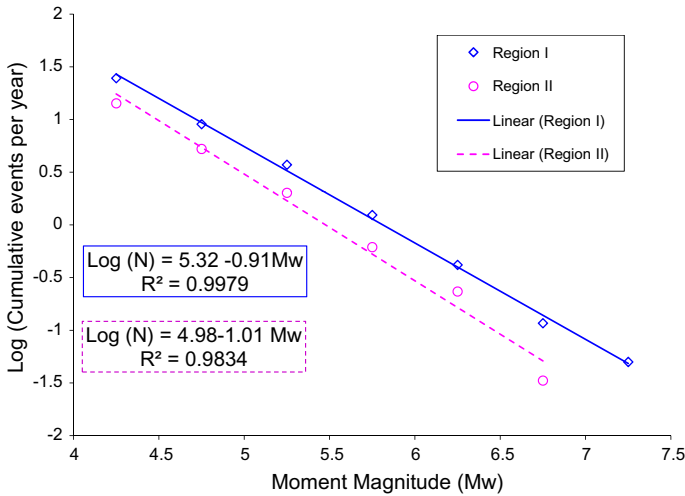


Fig. 5 Gutenberg–Richter relation for Regions I and II

Table 2 Comparison of ‘*b*’ parameter of the present study with previous data

Region I	Region II
0.91 (present work)	1.01 (present work)
0.86 (Kumar et al. 2013)	0.80 (Kumar et al. 2013)
0.73 (NDMA 2010)	0.81 (NDMA 2010)
1.0 (Sreevalsa et al. 2011)	0.85 (Sreevalsa et al. 2011)
0.80 (Mahajan et al. 2010)	
0.65 (Kumar 2012)	

6 Maximum probable earthquake magnitude (M_{max}) and focal depth

The maximum probable earthquake magnitude is defined as the upper limit of earthquake magnitude for a given region and is synonymous with the magnitude of the largest possible earthquake (EERI Committee on Seismic Risk 1984; Working Group on California Earthquake Probabilities 1995). It assumes a sharp cutoff magnitude at a maximum magnitude, M_{max} , so that, by definition, no earthquakes are to be expected with magnitude exceeding M_{max} (Joshi and Sharma 2008). The maximum magnitude regarding each fault has been calculated using three methods mentioned below:

1. Kijko and Sellevoll (1989) have proposed a method to estimate maximum magnitude considering doubly truncated Gutenberg–Richter relation. This method is only valid when β for the region is known (CASE I; Kijko and Sellevoll 1989).

$$M_{max} = m_{max}^{obs} + \frac{E_1(n_2) - E_1(n_1)}{\beta \exp(-n_2)} + m_{min} \exp(-n) \tag{2}$$

where M_{max} is the largest possible earthquake magnitude, m_{max}^{obs} is the maximum observed magnitude on each fault, n is the total earthquakes above magnitude of completeness

- $(m_{\min}), n_1 = n/\{1 - \exp[-\beta(m_{\max} - m_{\min})]\}, n_2 = n_1\{ \exp [-\beta(m_{\max} - m_{\min})]\}, E_1(\cdot)$ denotes an exponential integration function, which can be estimated as $E_1(z) = \frac{z^2+a_1z+a_2}{z(z^2+b_1z+b_2)} \exp(-z)$, where $a_1 = 2.334733, a_2 = 0.250621, b_1 = -3.330657$ and $b_2 = -1.681534$ (Abramowitz and Stegun 1970), m_{\max}^{obs} for each fault and m_{\min} , the value of M_{\max} has been estimated using Eq. 2. For the estimation of M_{\max}, m_{\min} is calculated as per the methods described by Woessner and Stefan (2005). Detailed description of calculating m_{\min} and ‘a’ and ‘b’ value for Patna region has been discussed in Anbazhagan et al. (2015). It has been observed that magnitude of completeness varies from 1.7 to 5 for Region I, but for Region II, it varies from 1.7 to 4.9. So taking that into account, $4.5 M_w$ has been taken as the minimum magnitude for further analysis for Regions I and II. This method for calculating M_{\max} has been widely used by various researchers worldwide as well as in India. In the present study area, regional values are used as per Kijko and Sellevoll (1989).
- M_{\max} has been also estimated by adding a constant value of 0.3 if the m_{\max}^{obs} is less than 5 (M_w) and add 0.5 for m_{\max}^{obs} greater than 5 to the m_{\max}^{obs} value of each fault similar to NDMA (2010).
 - M_{\max} is also estimated using regional rupture characteristics by considering the maximum magnitude observed and possible seismic source of SSA. The whole procedure to find region-specific rupture characteristic was presented in Anbazhagan et al. (2013b, 2014). The same procedure is followed for determining M_{\max} for each seismic source (see Fig. 3). Subsurface rupture length (RLD) of each seismic source has been estimated by using well-accepted correlation between RLD and M_w by Wells and Coppersmith (1994) from the maximum observed magnitude of each source. Percentage fault rupture (PFR) which is the ratio of subsurface rupture length (RLD) to total fault length (TFL) is expressed in percentage. As per Fig. 6, the plotting of PFR against TFL shows that PFR follows a unique trend for interplate region. Possible worst scenario PFR is established by considering minimum, maximum and average PFR in four length bins as shown in Table 3. For each length bin, PFR for worst scenario earthquake has been taken as five times the average PFR, which is also more

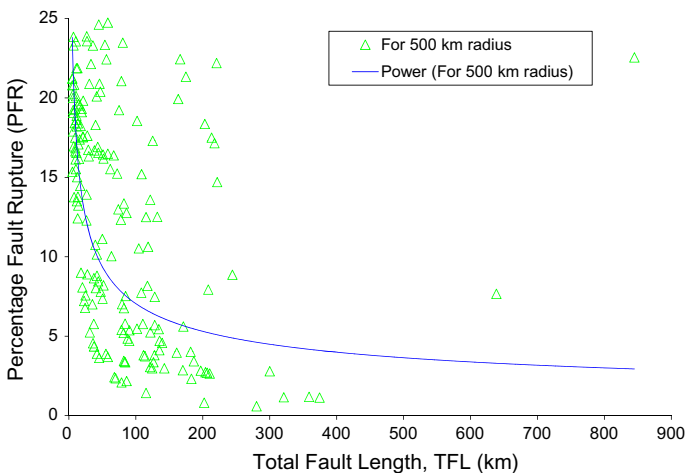


Fig. 6 Regional rupture characters for Patna

Table 3 Regional rupture character for various distance bins

Length bins	PFR (% TFL)			PFR (% TFL) for worst scenario (WS)	Ratio of PFR for WS to maximum PFR
	Maximum	Minimum	Average		
<100	25	4.71	15.06	33	1.32
100–300	22.2	2.32	8.74	32	1.44
300–600	3	1.13	1.56	5.5	1.83
>600	22.55	7.67	15.11	25	1.11

than the maximum reported PFR. PFR for the worst scenario (see Table 3) is taken as the regional rupture character of the seismic study area. The subsurface rupture length is calculated based on the length of each source, which is further used to estimate the M_{\max} of each source using well-established Wells and Coppersmith (1994) relationship. The whole procedure is explained in Anbazhagan et al. (2015).

The absolute M_{\max} for each source has been calculated from the above-mentioned three approaches. Table 4 gives the M_{\max} value from the seismic source having an estimated maximum magnitude greater than 6.5. So the final M_{\max} for each source was taken as maximum from these three approaches and given in the last column of Table 4.

6.1 Focal depth of earthquake

Determination of focal depth of future earthquake is an indispensable and complicated job for seismic hazard analysis. Comprehension about the depth division of the diffuse seismicity (i.e., derived from the seismology database) should be included in the seismic hazard analysis (Anbazhagan et al. 2013b). Most of the studies regarding seismic hazard analysis incorporate the lowest focal depth or depth considering the minor earthquakes (Anbazhagan et al. 2013b). In the present study, whole catalogue has been analyzed for the determination of the appropriate focal depth of future earthquake. Hence, focal depth is analyzed with magnitude and epicentral distance for Patna SSA. Figure 7 shows the plot of depth versus epicenter distance of the events having a moment magnitude between 5 and 6 and greater than 6 for the whole Patna region. Depth of earthquakes having a moment magnitude less than 5 is not considered because M_{\max} of all sources are 5 and above. It has been seen from Fig. 7 that for a moment magnitude between 5 and 6, focal depth varies from 5 to 75 km, whereas for moment magnitude greater than 6, it varies from 10 to 75 km for the 500 km as epicentral distance. Considering the worst-case scenario, focal depth of 10 km is adopted for epicenter distance up to 200 km (marked in Fig. 7) for all the magnitude and focal depth of 5 km is taken for $M_w < 6$ and 10 km for $M_w > 6$ beyond an epicenter distance of 200 km as per Fig. 7.

7 Ground motion prediction equation (GMPE)

Ground shaking through an earthquake is accountable for the structural damage and ground failures either within the epicentral region or at far distances. The region-specific GMPE is an important component in the seismic hazard analysis for both seismic macro- and

Table 4 M_{max} values from three approaches and assigned M_{max} value for each source

Seismic source	Observed magnitude (M_w)	Regional rupture characteristics			By incremental value	Kijko and Sellevoll (1989)	M_{max} taken for hazard analysis
		TFL (km)	RLD (% TFL) ^a	M_{max}			
MBT	8	844.92	211.23	8.1	8.5	8	8.5
MCT	7	638.78	159.7	7.9	7.5	7	7.9
S01	5.4	135.37	43.32	6.9	5.9	5.4	6.9
S02	5.4	206.58	66.1	7.2	5.9	5.4	7.2
S03	5.2	183.13	58.6	7.1	5.7	5.2	7.1
S05	5.2	142.64	45.65	6.9	5.7	5.2	6.9
S06	5.8	128.34	41.07	6.9	6.3	5.9	6.9
S07	5.8	58.19	19.2	6.3	6.3	6.6	6.6
S08	4.5	202.28	64.73	7.2	4.8	4.5	7.2
S09	5.6	128.31	41.06	6.9	6.1	5.6	6.9
S10	6	118.41	37.89	6.8	6.5	6	6.8
S104	5.4	101.82	32.58	6.7	5.9	5.5	6.7
S105	6.8	166.32	53.22	7.1	7.3	6.8	7.3
S106	6.8	213.24	68.24	7.2	7.3	6.8	7.3
S109	6.7	163.44	52.3	7	7.2	6.7	7.2
S11	5.6	181.92	58.22	7.1	6.1	5.6	7.1
S111	6	53.94	17.8	6.3	6.5	7	7
S112	6.2	78.44	25.89	6.5	6.7	6.3	6.7
S12	6.4	125.31	40.1	6.9	6.9	6.4	6.9
S125	5.8	77.77	25.66	6.5	6.3	6.6	6.6
S128	6.4	244.38	78.2	7.3	6.9	6.4	7.3
S13	5.2	126.41	40.45	6.9	5.7	5.2	6.9
S130	6.8	203.22	65.03	7.2	7.3	6.8	7.3
S131	5.3	90.58	29.89	6.6	5.8	5.4	6.6
S139	5.6	134.34	42.99	6.9	6.1	5.6	6.9
S14	5.1	124.58	39.87	6.8	5.6	5.2	6.8
S141	6.2	108.66	34.77	6.7	6.7	6.3	6.7
S146	5.3	127.89	40.92	6.9	5.8	5.3	6.9
S15	5.5	161.13	51.56	7	6	5.6	7
S157	5.8	117.45	37.58	6.8	6.3	5.9	6.8
S158	5.5	84.81	27.99	6.6	6	5.7	6.6
S16	5.5	110.65	35.41	6.8	6	5.6	6.8
S161	6.2	208.22	66.63	7.2	6.7	6.2	7.2
S17	5.1	121.48	38.87	6.8	5.6	5.2	6.8
S172	5.2	113.76	36.4	6.8	5.7	5.2	6.8
S18	5.5	121.87	39	6.8	6	6.1	6.8
S19	5.5	186.75	59.76	7.1	6	5.5	7.1
S20	5.5	139.32	44.58	6.9	6	5.5	6.9
S25	4.5	280.49	89.76	7.4	4.8	4.5	7.4
S27	5.4	82.36	27.18	6.6	5.9	5.6	6.6
S28	5.2	111.79	35.77	6.8	5.7	5.2	6.8

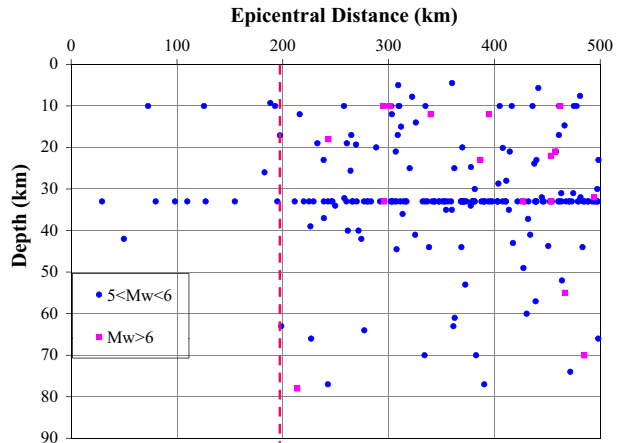
Table 4 continued

Seismic source	Observed magnitude (M_w)	Regional rupture characteristics			By incremental value	Kijko and Sellevoll (1989)	M_{max} taken for hazard analysis
		TFL (km)	RLD (% TFL) ^a	M_{max}			
S31	5.2	90.25	29.78	6.6	5.7	5.3	6.6
S32	5.2	87.61	28.91	6.6	5.7	5.7	6.6
S33	5.9	86.13	28.42	6.6	6.4	6.2	6.6
S34	5.4	197.04	63.05	7.2	5.9	5.4	7.2
S35	4.5	115.3	36.89	6.8	4.8	4.5	6.8
S36	5.5	135.63	43.4	6.9	6	5.5	6.9
S39	5.2	81.66	26.95	6.6	5.7	5.3	6.6
S43	4.6	86.35	28.49	6.6	4.9	4.7	6.6
S44	5.3	170.39	54.52	7.1	5.8	5.3	7.1
S45	6.8	217.61	69.63	7.3	7.3	6.8	7.3
S47	4.8	27.72	9.15	5.8	5.1	8	8
S48	5.3	84.09	27.75	6.6	5.8	5.4	6.6
S49	5.7	108.2	34.62	6.7	6.2	5.8	6.7
S50	6.1	115.38	36.92	6.8	6.6	6.1	6.8
S52	5.9	82.28	27.15	6.6	6.4	6	6.6
S53	5.9	104.4	33.41	6.7	6.4	6	6.7
S54	6.2	132.04	42.25	6.9	6.7	6.2	6.9
S57	6.7	221.6	70.91	7.3	7.2	6.7	7.3
S58	5.4	204.19	65.34	7.2	5.9	5.4	7.2
S59	6.8	174.9	55.97	7.1	7.3	6.8	7.3
S60	5.4	210.41	67.33	7.2	5.9	5.4	7.2
S62	7	220.63	70.6	7.3	7.5	7	7.5
S63	6.3	80.58	26.59	6.6	6.8	6.5	6.8
S64	4.9	82.04	27.07	6.6	5.2	5	6.6
S69	6.2	121.58	38.9	6.8	6.7	6.3	6.8
S73	6.3	101.99	32.64	6.7	6.8	6.5	6.8
S76	6.1	74.98	24.74	6.5	6.6	6.1	6.6
S77	4.9	83.29	27.49	6.6	5.2	5.1	6.6
S78	6.1	58.28	19.23	6.3	6.6	7.2	7.2
S82	4.9	84.24	27.8	6.6	5.2	5	6.6
S83	5.8	171.1	54.75	7.1	6.3	5.8	7.1
S90	5.8	61.81	20.4	6.4	6.3	6.6	6.6

^a Calculated as per Table 3

microzonation. Developed countries are working on the next generation of ground motion attenuation (NGA) for the better prediction of ground shaking due to any future earthquake events (Campbell and Bozorgnia 2006; Kaklamanos and Baise 2011). But the limited number of GMPEs is available for seismic hazard estimation, both in bedrock as well as at surface by accounting the local site effects in India and other parts of the world (Atkinson and Boore 2006; NDMA 2010). An indispensable step in hazard analysis for any region is the selection of appropriate GMPE for forecasting the ground shaking.

Fig. 7 Distribution of focal depth of earthquake with epicentral distance



Various researchers have analyzed the attenuation characteristics of the Himalayan region based on the available data. Region-specific GMPEs developed by Singh et al. (1996), Sharma (1998), Nath et al. (2005, 2009), Das et al. (2006), Sharma and Bungum (2006), Baruah et al. (2009), Sharma et al. (2009), Gupta (2010), NDMA (2010) and Anbazhagan et al. (2013a) are based on recorded as well as simulated earthquake data. Table EM1 (submitted as electronic material) summarizes various GMPEs developed in different parts of the Himalayan belt along with the range of magnitude and distance to which each GMPE is valid for. In addition to these GMPEs, there are several GMPEs developed for similar tectonic conditions, which can also be applicable to the Himalayan region. GMPEs developed elsewhere and applicable to Himalayan regions are Abrahamson and Litehiser (1989), Youngs et al. (1997), Campbell (1997), Spudich et al. (1999), Atkinson and Boore (2003), Takahashi et al. (2004), Ambraseys et al. (2005), Kanno et al. (2006), Zhao et al. (2006), Campbell and Bozorgnia (2008), Idriss (2008), Boore and Atkinson (2008), Abrahamson and Silva (2007), Aghabarti and Tehranzadeh (2009), Lin and Lee (2008) and Akkar and Bommer (2010). Table EM2 (submitted as electronic material) shows summary of 16 applicable GMPEs for Himalayan region. The list of GMPE applicable for the study region along with abbreviations is given in Table 5. Figure 8 shows the plot of region-specific available GMPEs and applicable GMPEs for M_w 6.8 and hypocenter distance of 10–500 km. From Fig. 8, it may be difficult to identify the appropriate region-specific GMPEs for the hazard analysis by comparison.

The seismic hazard assessment requires appropriate selection of GMPEs, which will help to forecast representative level of ground shaking (Bommer et al. 2010). The selected GMPE should be capable of apprehending the essence of ground motion, i.e., earthquake source, path and site attributes at the same time. GMPE developed from the past four decades has shown rather consistency in the related inconsistency and epistemic uncertainty, notwithstanding the increasing complexities (Strasser et al. 2009; Douglas and Mohais 2009; Douglas 2010; Nath and Thingbaijam 2011; Anbazhagan et al. 2013b). This gives rise to the obligation of the selection and ranking of GMPEs (Bommer et al. 2005; Cotton et al. 2006; Sabetta et al. 2005; Scherbaum et al. 2004, 2005; Hintersberger et al. 2007; Nath and Thingbaijam 2011) and which results in usage of multiple GMPEs in a logic tree framework for hazard analysis. Many researchers in India generally use two or three GMPEs for predicting the hazard values without any physical and mathematical

Table 5 Available GMPEs with their abbreviations considered for the seismic study area

S. No.	Ground motion prediction equation (GMPE)	Abbreviation of the equations
1.	Singh et al. (1996)	SI-96
2.	Sharma (1998)	SH-98
3.	Nath et al. (2005)	NATH-05
4.	Das et al. (2006)	DAS-06
5.	Sharma and Bungum (2006)	SHBU-06
6.	Baruah et al. (2009)	BA-09
7.	Nath et al. (2009)	NATH-09
8.	Sharma et al. (2009)	SH-09
9.	Gupta (2010)	GT-10
10.	National Disaster Management Authority (2010)	NDMA-10
11.	Anbazhagan et al. (2013a, b)	ANBU-13
12.	Abrahamson and Litehiser (1989)	ABLI-89
13.	Youngs et al. (1997)	YONG-97
14.	Campbell (1997)	CAMP-97
15.	Spudich et al. (1999)	SPUD-99
16.	Atkinson and Boore (2003)	ATKB-03
17.	Takahashi et al. (2004)	TAKA-04
18.	Ambraseys et al. (2005)	AMB-05
19.	Kanno et al. (2006)	KANO-06
20.	Zhao et al. (2006)	ZHAO-06
21.	Campbell and Bozorgnia (2008)	CABO-08
22.	Idriss (2008)	IDRS-08
23.	Boore and Atkinson (2008)	BOAT-08
24.	Abrahamson and Silva (2007)	ABSI-08
25.	Aghabarati and Tehranizadeh (2009)	AGTE-08-09
26.	Lin and Lee (2008)	LILE-08
27.	Akkar and Bommer (2010)	AKBO-10

reasoning; however, considering 2–3 GMPE randomly and comparing with the observed value may give inconsistent results because of the absence of comprehensive procedure (Delavaud et al. 2012). Hence, for the present study area, the best-suited GMPE is selected for hazard analysis considering past earthquake data.

The best-suited GMPE has been selected considering the criteria proposed by Bommer et al. (2010) and by performing the efficacy test recommended by Scherbaum et al. (2009) and Delavaud et al. (2009). The determination of order of ranking of GMPEs is based on the observed earthquakes in a particular region. In the present study, the information-theoretic approach recommended by Scherbaum et al. (2009) has been used. The efficacy test makes use of average sample log-likelihood (LLH) for the ranking purpose of the available GMPE of a particular SSA. The efficacy test using average LLH has been performed successfully by Delavaud et al. (2009) and applied to India by Nath and Thingbaijam (2011). Hence, for the present study, efficacy test has been carried out by considering macroseismic intensity map of 1833 and 1934 Bihar–Nepal earthquake (shown in Fig. 1a, b) and PGA-European Macroseismic Scale (EMS, Grünthal 1998) relation

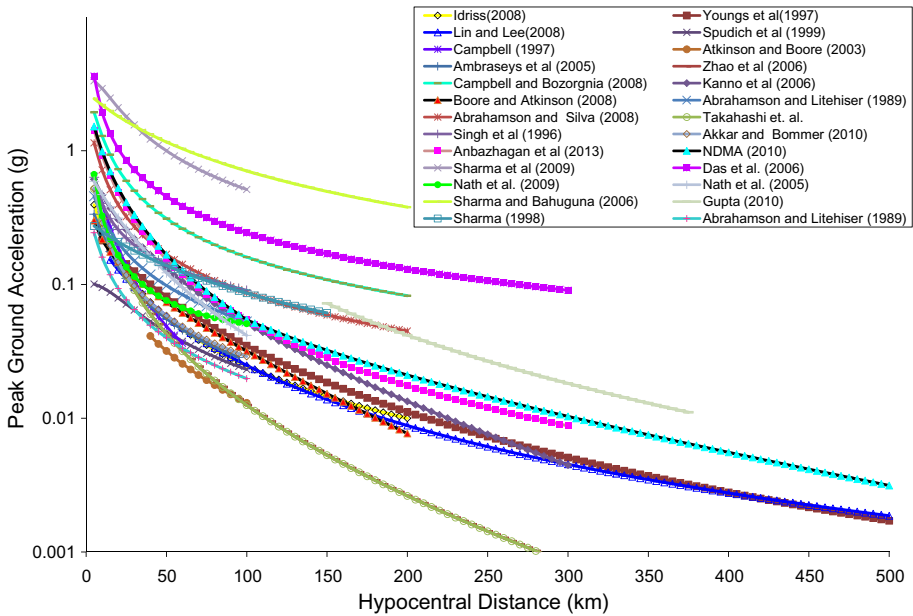


Fig. 8 Comparison of ground motion prediction equations applicable to Himalayan region for earthquake moment magnitude of 6.8

proposed by Nath and Thingbaijam (2011) for Indian crustal earthquakes. The LLH is calculated using the equation given by Delavaud et al. (2009) and given as Eq. 3.

$$LLH(g, x) = -\frac{1}{n} \sum_{i=1}^N \log_2(g(x_i)) \tag{3}$$

where $x = \{x_i\}$, $i = 1, \dots, N$ are the empirical data and $g(x_i)$ is the likelihood that model g has produced for the observation x_i . In this case of GMPE selection, g is the probability density function given by a GMPE to predict the observation produced by an earthquake with magnitude M at a site i that is located at a distance R from the source (Delavaud et al. 2012).

The PGA variation with distance of all the applicable GMPEs has been discussed (see Fig. 8). Based on the trend of variation, the hypocentral distance is divided into three length bins as 0–100, 100–300 and 300–500 km. For the hazard analysis, the ranking of GMPE has been considered for all the three bins. As macroseismic intensity map for 1934 earthquake is available up to 300 km, so for more than 300 km, 1833 earthquake has been considered for ranking of GMPEs. Some of the GMPEs such as Singh et al. (1996), Sharma (1998), Das et al. (2006), Baruah et al. (2009), Sharma et al. (2009) and Gupta (2010) are not used for efficacy test as the isoseismal map used in the present study area has a magnitude greater than 7.6 M_w . The LLH values along with the ranking of GMPEs are given in Table 6. The EMS values are used to estimate the LLH values and data support index (DSI), which are further used to rank the GMPEs. LLH values are not a measure of closeness, but a measure of the distance between a model and the data-generating process (Delavaud et al. 2012). Delavaud et al. (2012) have given a data support index (DSI) to know the percentage by which the weight on a model is increased or decreased through

data. DSI of an equation (given as Eq. 5) shows the percentage increase or decrease of weight of a model with respect to its state of non-informativeness (Delavaud et al. 2012).

$$w_i = \frac{2^{-\text{LLH}(g_i, x)}}{\sum_{k=1}^n 2^{-\text{LLH}(g_k, x)}} \quad (4)$$

$$\text{DSI}_i = 100 \frac{w_i - w_{\text{unif}}}{w_{\text{unif}}} \quad (5)$$

where $w_{\text{unif}} = 1/M$ and M are the number of models used for the calculation of LLH value.

Segmented-based ranking of GMPEs has been attempted in order to avoid over/underestimation of the PGA of shorter and longer distances. To select the best-suited GMPEs for each region past earthquake location, a DSI criterion has been used. For each distance segment, positive DSI values are identified and ranked based on maximum to minimum values. A maximum positive DSI value is considered first rank, and minimum is considered as lowest rank. Positive DSI values for different GMPEs for Patna SSA are marked as bold in Table 6. This study shows that GMPE developed by ANBU-13, NDMA-10 and KANO-06 is best suitable up to 100 km, and ANBU-13, NDMA-10, KANO-06 and BOAT-10 are best suitable for 100–300 km distances. GMPE given by NDMA-10 is only suitable GMPE for distance above 300 km and up to 500 km. These LLH values are further used to evaluate the LLH-based weight factor as per Delavaud et al. (2012) as it infers to what extent the data increase or decrease the weight of model with respect to the non-informativeness (see Table 6). In the present study, DSI is directly calculated using LLH and weight is calculated later from only those GMPE having positive DSI. The weight factor corresponds to particular GMPE for different segments are further used in evaluating the hazard of Patna SSA. Seismic hazard values in terms of PGA and SA can be calculated considering these equations for each seismic source.

8 Hazard maps for Patna region

To derive the hazard value, deterministic seismic hazard analysis (DSHA) and probabilistic hazard seismic hazard (PSHA) analysis have been widely practiced. In this study, both PSHA and DSHA have been used to estimate the peak ground acceleration (PGA) and spectral acceleration (SA) based on past seismicity and future maximum magnitude. The detailed procedures for both the methods are given in Anbazhagan et al. (2009) and Kumar et al. (2013). These hazard maps are most widely used for significant structures and seismic disaster planning and mitigation. GMPEs have been selected, and weights are calculated based on regional data. The weight factor was 0.53, 0.35 and 0.12 for ANBU-13, NDMA-10 and KANO-06, respectively, up to 100 km, and 0.32, 0.30, 0.22 and 0.16 for GMPEs of KANO-06, ANBU-13, NDMA-10 and BOAT-08 for segmented hypocentral distance of 100–300 km and a factor of 1 for NDMA-10 for more than 300 km hypocentral distance. Separate MATLAB code has been generated to determine PGA deterministically and probabilistically by considering magnitude, source-to-site distance and site condition. These codes have been validated with the results of EM-1110 (1999). The whole Patna district's SSA has been divided into 2500 grids of size $0.022^\circ \times 0.014^\circ$ along the longitude and latitude, respectively. Following procedure has been used to determine the PGA value for each of 2500 grids. Kriging interpolation technique has been used for the estimation of intermediate values of PGA for the development of the seismic hazard map.

8.1 Deterministic seismic hazard analysis (DSHA)

Usually in DSHA, one or more earthquakes are identified by magnitude and location with respect to site. In this approach, the earthquake is assumed to occur in the portion of the site closest to the site. In the present study, the hazard map of Patna district center has been prepared considering the entire seismic source with corresponding maximum magnitudes and systematically selected GMPEs having different weight factors. In total, 178 seismic sources have been found, which have experienced an earthquake magnitude of 4 and within 500 km radial distance around Patna (shown in Fig. 3). A MATLAB code has been developed for the DSHA, which has also been verified with the manual calculation of Patna district center. The minimum hypocentral distance has been estimated from the center of each grid to each fault using the code. The Patna SSA has been divided into 2500 grids of size $0.022^\circ \times 0.014^\circ$ along the longitude and latitude, respectively. The peak ground acceleration at each grid has been estimated considering the maximum magnitude and GMPE. The maximum PGA from the entire 178 seismic source will be assigned as the PGA for that grid. The similar technique has been adopted for all the 2500 grids for the development of new seismic hazard map of Patna. Kriging interpolation technique has been used for the estimation of intermediate values of PGA for the development of the seismic hazard map. Figure 9 shows the worst-case map of the Patna city center. The PGA variation has been found to be 0.14 g in the central part of Patna district, whereas it increased to 0.5 g in northwestern periphery. The high hazard values are resulted due to location of East Patna Fault and West Patna Faults within the city. In addition to that, spectral acceleration (SA) maps at 0.2 and 1 s have been developed and shown in Figs. 10 and 11. The weight factor used for SA calculation is similar to PGA calculations. This is because of limited data available in determining the weight factor for the SA hazard map at 0.2 and 1 s, but in future, this may be taken into consideration as these weight factors have different impact at different periods. Areas like Nehru Nagar, Patna High Court, Kothia, Pataupura Colony, Makhdhumpur and surrounding areas are less prone to earthquake-

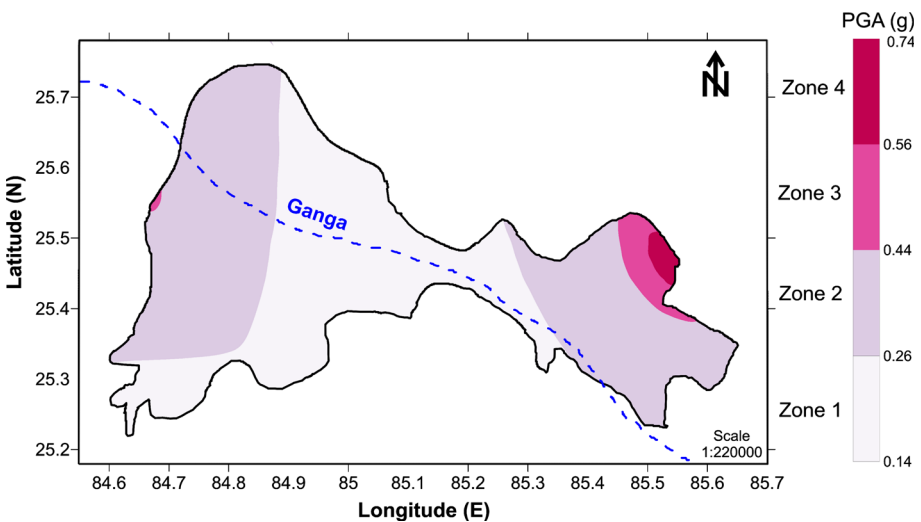


Fig. 9 Peak ground acceleration (PGA) map of Patna urban center

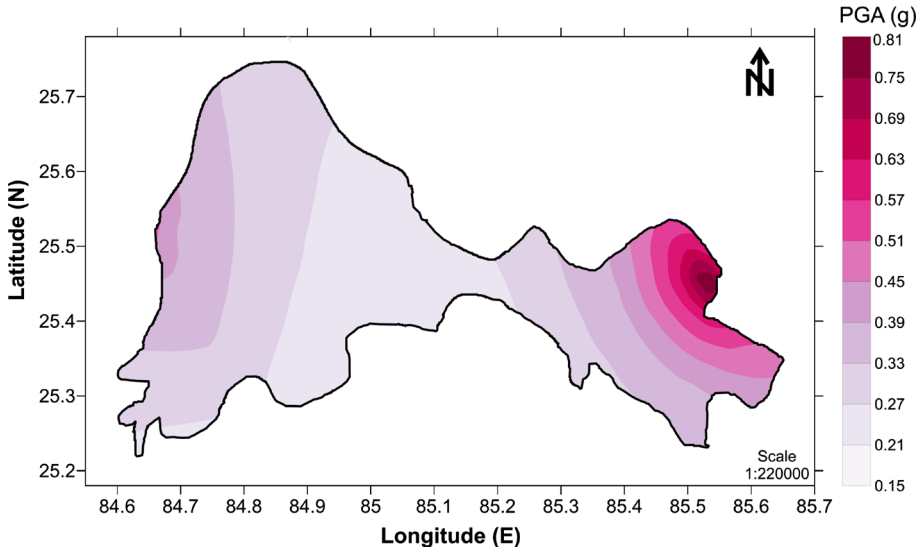


Fig. 10 Spectral acceleration at 0.2 s map of Patna urban center

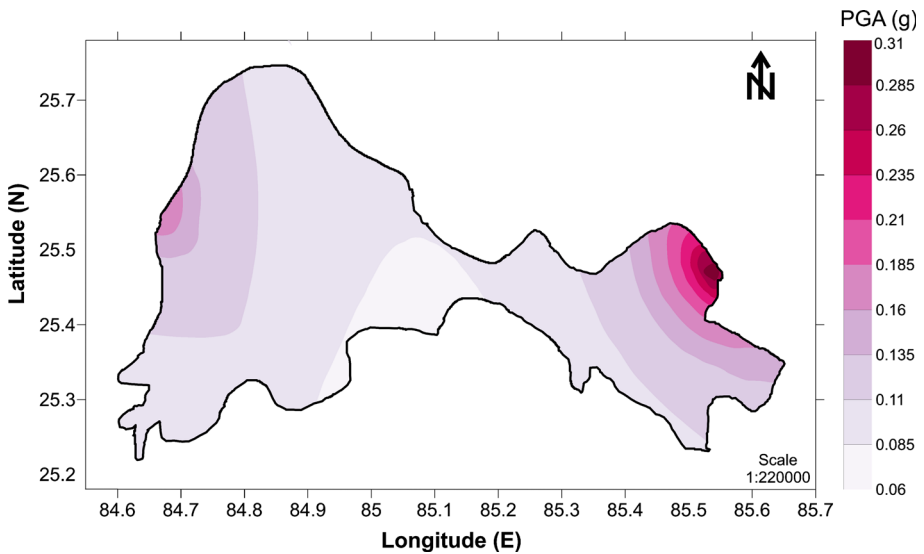


Fig. 11 Spectral acceleration at 1 s map of Patna urban center

induced ground shaking; however, places near and surrounding Hanuman Nagar, Sadhanpuri, Vighrahpur, Loknayaak Jaiprakash Airport, Bihar Chak, Patrakar Nagar are more susceptible to earthquake shaking. Since, these levels of ground shaking are evaluated at bedrock level, and no changes in PGA contours along the alignment of river Ganga can be seen here. The large variation in PGA value within the city may be due to Monghyr–Saharsa Ridge (see Fig. 2), Gandak Fault (S161), East Patna Fault (S59) and West Patna

Fault (S60) as they located within the southeastern part of the city. The maximum PGA from DSHA for the present study is found to be 0.74 g. Parvez et al. (2003) developed the DSHA Map for the entire Indian subcontinent and found PGA range between 0.3 and 0.6 g for the Patna city. However, the PGA value found from the present study is higher than that of deterministic seismic hazard macrozonation carried out by Kolathayar et al. (2012), which is in the range of 0.15–0.25 g.

8.2 Probabilistic seismic hazard analysis (PSHA)

The probability of exceedance of a given ground motion in a particular time period can be estimated once the probability of its size, locations and level of ground shaking is known cumulatively. The seismic hazard map for Patna has been generated using PSHA using probabilistic method proposed by Cornell (1968), which was later improved by Algermissen et al. (1982). For evaluating the seismic hazard using the classical approach (Cornell 1968), the entire SSA of Patna has been divided into 2500 grids of size $0.022^\circ \times 0.014^\circ$. The uncertainties associated with magnitude, hypocentral distance and probability of exceedance for GMPEs for 178 seismic sources have been computed using a program developed in MATLAB. The program computed the frequency of exceedance of a particular magnitude ' m_i ' occurring at a particular hypocentral distance ' R ' with a known probability of exceedance with respect to ' z ', and the combined frequency of exceedance of a particular ground motion can be estimated by merging all types of uncertainties for each seismic source. The detailed methodology for determining the PGA using probability seismic hazard analysis is explained in Anbazhagan et al. (2009) in this journal.

A hazard curve, which is defined as the frequency of exceedance of various levels of ground motion for 10 most vulnerable sources at Patna center, is shown in Fig. 12. It can be seen from Fig. 12 that S60 (West Patna Fault) is the most vulnerable source located at a hypocentral distance of 55.11 km with a maximum magnitude of 7.5 (M_w). Other sources, which have been found vulnerable for Patna, are also shown in Fig. 12 as S139, S58, S61, S57, S138, S62, S39, S54 and S20. The hazard curve for any SSA can be obtained by the summation of all the hazard curves obtained from all the active sources. Thus, merging all the hazard curves from 178 sources at the Patna center will give the hazard curve for Patna district center. Figure 13 shows the cumulative hazard curve obtained at the Patna district

Fig. 12 Hazard curve for ten most contributing seismic source at Patna

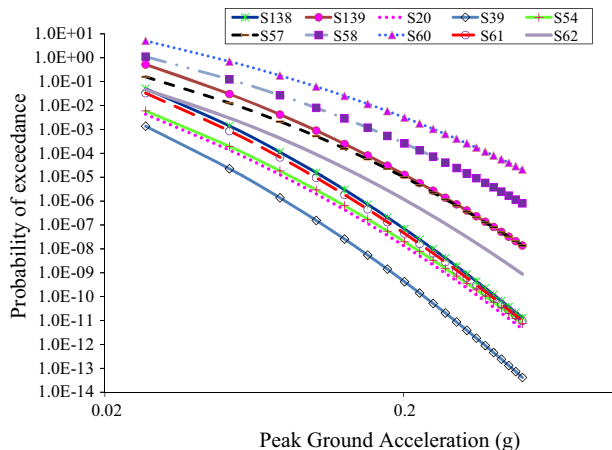
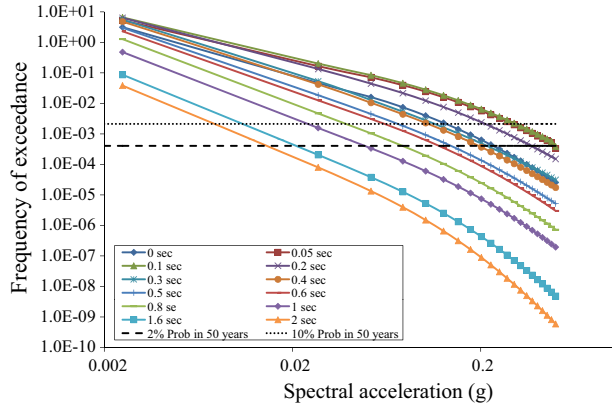


Fig. 13 Hazard curve at Patna for different periods using classical approach



center for 0, 0.05, 0.1, 0.2, 0.3, 0.4, 0.6, 0.8, 1.0, 1.6 and 2 s. Hazard curve subsequent to different periods presents the spectral acceleration values for an identified probability of exceedance in a particular time period. In can be observed from Fig. 13 that the frequency of exceedance for 0.075 g at zero second is 0.0074311, which will give the return period 135 years (return period is the inverse of the frequency of exceedance). This indicates that PGA of 0.075 g has a 31.03 % probability of exceedance in 50 years at the Patna center. Similarly, for 0.5 g, the frequency of exceedance at zero seconds is 2.55E–05, which will give a return period of 39.2 thousand years or a probability of exceedance of 1.28×10^{-1} % in 50 years at Patna city center. As the period on interest increases from zero second to 0.8 s, a huge change in return period has been observed from Fig. 13. Initially, the frequency of exceedance decreases from 135 years at zero periods to 22 years in 0.1 s, which further increases to 46 years in 0.2 s and again till 2.53E + 05 years for 2 s. In order to understand the hazard contribution from various combinations of magnitude and hypocentral distance, degradation plot is generated, which is a function of magnitude and hypocentral distance for all the levels of spectral period associated with the GMPEs. The mean degradation plot for Patna SSA for 2 and 10 % probability of exceedance at 50 years have been made in order to understand the hazard contribution for various magnitudes at a different hypocentral distance and are shown in Fig. 14a, b. It has been observed from Fig. 14 that the motion for 6.0 M_w at 40 km hypocentral distance is predominant for 2 % probability of exceedance at 50 years. Similarly, for 10 % probability of exceedance at 50 years, the motion for 5.5 M_w at 50 km hypocentral distance is predominant. Hazard curve has been generated at each grid for Patna SSA; the level of ground motion for frequency of exceedance ' $\nu(z)$ ' can be determined from it. The level of ground motions has been estimated from the zero period hazard curves (PGA value) of each grid for 2 and 10 % probability of exceedance in 50 years. Figure 15a, b is the PSHA maps for Patna center for 2 and 10 % probability of exceedance in 50 years, respectively. It can be observed from Fig. 15a that PGA varies from 0.44 g in the northwestern and 0.4 g in the north eastern periphery to 0.08 g toward the central part. PGA value in the southeastern part of Patna is 3–4 times as compared to southwestern part. Similarly, for 10 % probability of exceedance in 50 years, PGA value is low at the central part of the city and increases about fivefold toward the northeastern part of the city. In addition to that, spectral acceleration at, respectively, 0.2 and 1 s has been given as Fig. 16a–d for the return period of 2475 and 475 years, respectively. The increment is due to East Patna Fault (S59) and

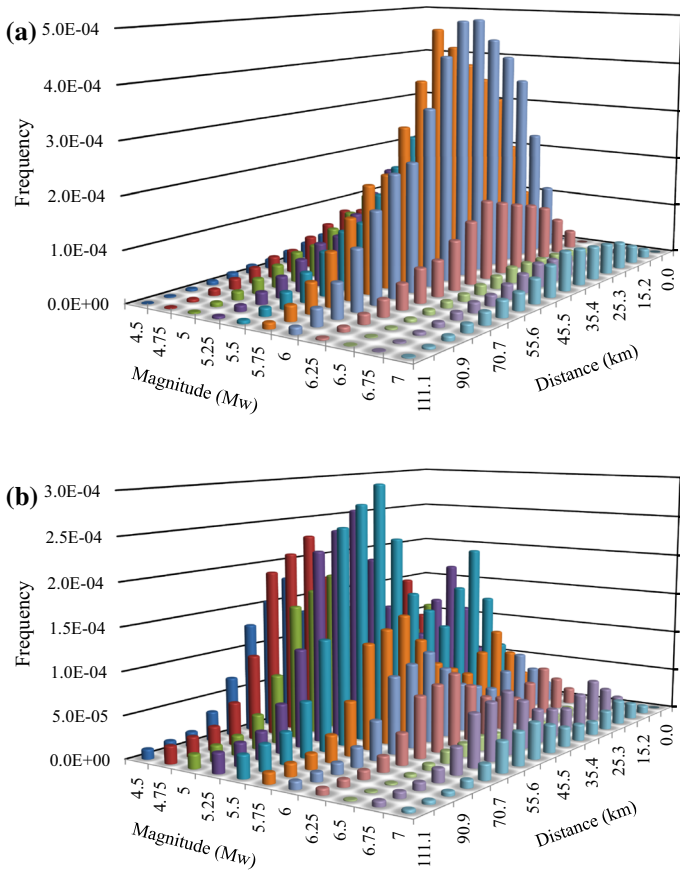


Fig. 14 **a** Deaggregation of hazard value at Patna at bed rock at PGA for 2 % probability of exceedance in 50 years, **b** deaggregation of hazard value at Patna at bed rock at PGA for 10 % probability of exceedance in 50 years

West Patna Fault (S60), which lie within the city and are source of devastating earthquakes. Southwestern part and central part include areas like Nehru Nagar, Patna High Court, Kothia, Pataupura Colony, Makhdhumpur and surrounding areas, which are less prone to earthquake-induced ground shaking. However, areas which fall in eastern and northern part of the city such as Hanuman Nagar, Sadhanpuri, Vighrahpur, Loknayaak Jai-prakash Airport, Bihar Chak, Patrakar Nagar and their nearby areas are more susceptible to earthquake shaking. Since these levels of ground shaking are evaluated at bedrock level, however, no changes in PGA contours along the alignment of river Ganga can be seen. Recently, National Disaster Management Authority (NDMA 2010) and Nath and Thingbaijam (2012) have developed a PSHA map for entire India. Nath and Thingbaijam (2012) predicted the PGA value at Patna considering 10 % probability of exceedance in 50 years as 0.13 g, whereas as per NDMA (2010), PGA value at 2 and 10 % probability of exceedance for 50 years was 0.08 and 0.04 g, respectively. Bhatia et al. (1999) presented a PSHA of India under the Global Seismic Hazard Assessment Program (GSHAP) framework. As per Bhatia et al. (1999), PGA value is in between 0.1 and 0.15 g of Patna

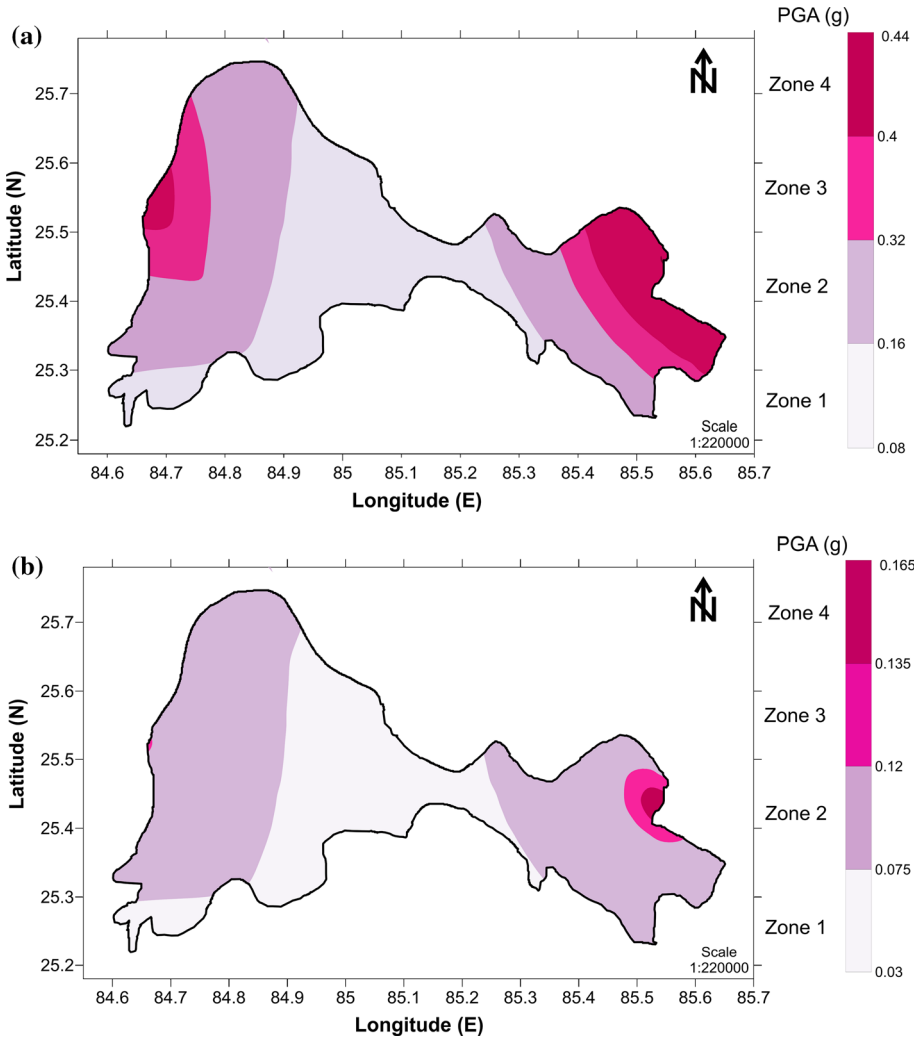


Fig. 15 **a** PSHA map for Patna district for 2 % probability of exceedance in 50 years, **b** PSHA map for Patna district for 10 % probability of exceedance in 50 years

considering 10 % probability of exceedance in 50 years. The predicted PGA value in this study is comparable and slightly higher than the previous studies, and it may be due to updated seismicity and considering regional-specific maximum magnitude and GMPE.

9 Site-specific spectrum

The site-specific design spectrum is necessary to design and to understand amplification character of the region. In the present study, design spectrum is derived from the GMPE as mentioned above with respect to different segments. For deriving the design spectrum, the

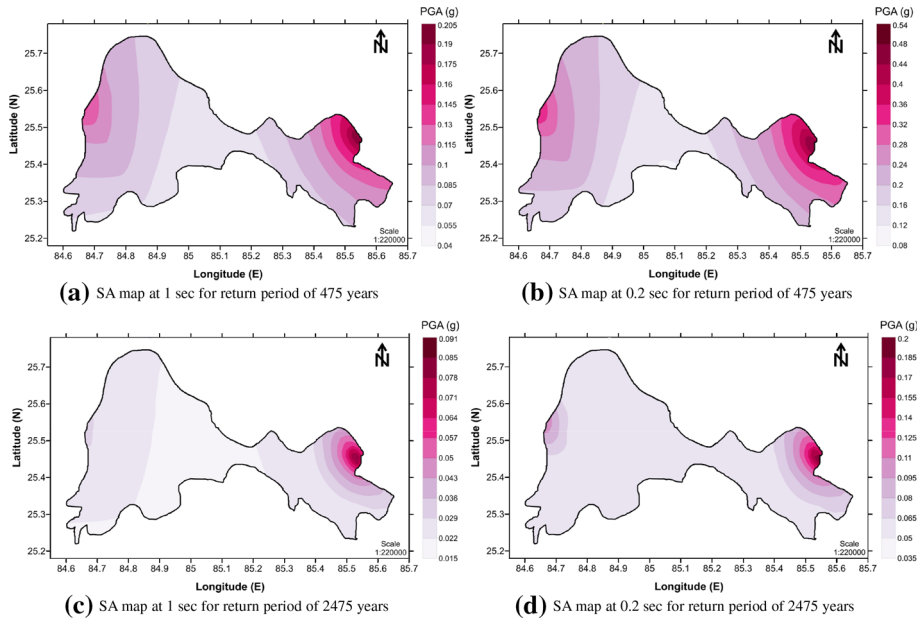


Fig. 16 **a** SA map at 1 s for 2 % probability of exceedance in 50 years, **b** SA map at 0.2 s for 2 % probability of exceedance in 50 years, **c** SA map at 1 s for 10 % probability of exceedance in 50 years and **d** SA map at 1 s for 10 % probability of exceedance in 50 years

whole district is divided into four zones based on PGA values calculated using DHSA results (see Fig. 9). These zones are Zone 1 ($0.14 \leq \text{PGA} < 0.26$), Zone 2 ($0.26 \leq \text{PGA} < 0.44$), Zone 3 ($0.44 \leq \text{PGA} < 0.56$) and Zone 4 ($\text{PGA} \geq 0.56$). Similarly, design spectrum (5 % damping) for 2 and 10 % probability of exceedance in 50 years has been developed by dividing the hazard map into four different zones in Fig. 15a, b. These zones are Zone 1 ($0.08 \leq \text{PGA} < 0.16$), Zone 2 ($0.16 \leq \text{PGA} < 0.32$), Zone 3 ($0.32 \leq \text{PGA} < 0.4$) and Zone 4 ($\text{PGA} \geq 0.4$) for a 2 % probability of exceedance in 50 years, and Zone 1 ($0.03 \leq \text{PGA} < 0.075$), Zone 2 ($0.075 \leq \text{PGA} < 0.12$), Zone 3 ($0.12 \leq \text{PGA} < 0.135$) and Zone 4 ($\text{PGA} \geq 0.135$) for a 10 % probability of exceedance in 50 years. For each of the zones, a spectral acceleration has been estimated at the center of the zone (which is similar for both PSHA and DSHA) from the valid GMPEs. The site-specific GMPEs ANBU-13, NDMA-10 and KANO-06 are used up to 100 km and ANBU-13, NDMA-10, BOAT-08 and KANO-06 from 100 to 300 km for deriving design spectra. Spectral acceleration which is a function of period for the respective GMPEs at 5 % damping has been taken from respected research papers. So, M_{\max} and the average shortest distance from each grid have been identified from the vulnerable seismic sources for developing design spectra at 5 % damping level. Averaged smoothed design spectrum has been developed as per Malhotra (2006). Design spectrum comprises of a peak, valley and shape variation in response spectrum from each GMPE. The design spectra are normalized with respect to spectral acceleration at zero periods (PGA) and shown as spectral ratio versus time period in Fig. 17. Figure 17a, b also shows the normalized design spectrum for 5 % damping for all the four zones considering DSHA values and PSHA with IS-code and Sikkim Earthquake spectrum comparison. This can be considered as the site-specific normalized design spectrum curve for 5 % damping at the rock level for all the four zones,

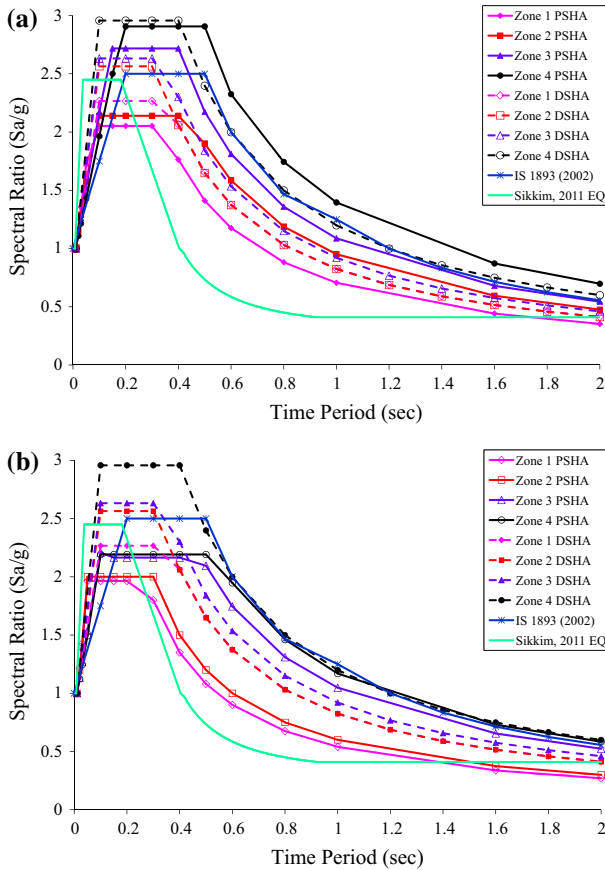


Fig. 17 **a** Normalized design spectrum for Patna for 5 % damping from four zones and spectrum from 2011 Sikkim earthquake and IS 1893 (2002) for 2 % probability of exceedance in 50 years comparing with worst-case scenario DSHA result, **b** normalized design spectrum for Patna for 5 % damping from four zones and spectrum from 2011 Sikkim earthquake and IS 1893 (2002) for 10 % probability of exceedance in 50 years comparing with worst-case scenario DSHA result

considering venerable seismic sources of Patna. These rock-level normalized design spectra have been compared with the 2011 Sikkim Earthquake recorded at Gangtok seismic station, located at rock site. It has been seen that present design spectrum hazard analysis is predicting slightly higher value than recorded values. It can be noted that the Sikkim earthquake magnitude is less than the maximum magnitude in the region. Site-specific spectrum developed for Patna is also compared with the design spectrum of IS-1893 (2002) of soil category of type I (Rock or Hard soil). The value of spectral acceleration developed from the present is low for zone 1 and higher for zone 2, 3 and 4 when compared with IS-1893 (2002) for larger period in case of DSHA, which may be because IS 1893 (2002) deals on a macrolevel (see Fig. 17a), and the present study is in microlevel and region specific. However, in case of PSHA considering 10 % probability, spectral acceleration is low for all the four zones, whereas in case of 2 % probability, high for zone 3 and zone 4 and low for zone 1 and zone 2. Additionally, the design calculated using DSHA is closely comparable with 2 % probability of exceedance in 50 years (see

Fig. 17a). It has been observed that normalized design spectra developed in this study both deterministically and probabilistically are either higher or lower as compared to IS-code. This might be due to incorporation of regional-specific parameters and using site-specific GMPE and maximum magnitude.

10 Conclusion

This paper presented seismic hazard map and site-specific design spectrum for Patna district both deterministically and probabilistically also considering region-specific data. A seismic study area of 500 km was arrived based on past earthquake damage distribution, and seismotectonic map has been generated. Seismotectonic map consists of declustered and homogenized past earthquake data and all the linear sources. The maximum magnitude has been estimated by considering three methods, i.e., incremental method, Kijko method and regional rupture-based characteristic. The maximum magnitude at each source was selected by considering the maximum of three methods. About 27 GMPEs are applicable to the study region, and suitable GMPES are identified for performing the efficacy test. The segmented-based efficacy test has been carried out, and GMPEs are selected. It was found that three GMPEs of ANBU-13, NDMA-10 and KANO-06 performed better up to 300 km epicentral distance and NDMA-10 for more than 300 km. Hazard curve for 0, 0.05, 0.1, 0.2, 0.3, 0.4, 0.6, 0.8, 1.0, 1.6 and 2 s has also generated. The hazard map for both 2 and 10 % probability of exceedance in 50 years has been developed. In addition to that spectral acceleration, hazard map has been developed at a period of 0.2 and 1 s for DSHA and PSHA. PGA varies from 0.14 to 0.74 g for DSHA, from 0.08 to 0.44 g in case for 2 % probability, and 0.03 to 0.165 g for 10 % probability. Furthermore, site-specific design spectrum developed using DSHA is comparable with 2 % probability of exceedance in 50 years; however, it is either low or high as compared to IS-code for DSHA as well as PSHA. The present result is slightly more advanced than previous studies and can be further used for estimating microzonation parameter of Patna district. Seismic hazard values given in this paper are at rock condition with $V_s^{30} > 1500$ m/s. These values may alter when site effects based on site-specific soil properties are considered.

References

- Abrahamson NA, Litehiser JJ (1989) Attenuation of vertical peak accelerations. *Bull Seismol Soc Am* 79:549–580
- Abrahamson NA, Silva WJ (2007) Abrahamson & Silva NGA ground motion relation for the geometric mean horizontal component of peak and spectral ground motion parameters. Report, Pacific Earthquake Research Center, Berkeley
- Abramowitz M, Stegun IA (1970) *Handbook of mathematical functions*, 9th edn. Dover Publication, New York
- Aghabarati H, Tehranizadeh (2009) Near-source ground motion attenuation relationship for PGA and PSA of vertical and horizontal components. *Bull Earthq Eng* 7:609–635. doi:10.1007/s10518-009-9114-9
- Akkar S, Bommer JJ (2010) Empirical equations for the prediction of PGA, PGV and spectral acceleration in Europe, the Mediterranean region and the Middle East. *Seismol Res Lett* 81:195–206
- Algermissen ST, Perkins DM, Thenhaus PC, Hanson SL, Bender BL (1982) Probabilistic estimates of maximum acceleration and velocity in rock in the contiguous United States. Open-File Report 82–1033. U.S. Geological Survey, Washington, DC, p 99
- Ambraseys NN, Douglas J (2004) Magnitude calibration of north Indian earthquakes. *Geophys J Int* 158:1–42

- Ambraseys N, Douglas JS, Sarma K, Smit PM (2005) Equation for the estimation of strong ground motions from shallow crustal earthquakes using data from Europe and the Middle East: horizontal peak ground acceleration and the spectral acceleration. *Bull Earthq Eng* 3:1–53
- Anbazhagan P, Vinod JS, Sitharam TG (2009) Probabilistic seismic hazard analysis for Bangalore. *Nat Hazards* 48:145–166
- Anbazhagan P, Vinod JS, Sitharam TG (2010) Evaluation of seismic hazard parameters for Bangalore region in South India. *Disaster Adv* 3(3):5–13
- Anbazhagan P, Kumar A, Sitharam TG (2012) Seismic site classification and correlation between standard penetration test N value and shear wave velocity for Lucknow city in Indo-Gangetic basin. *Pure Appl Geophys* 170(2013):299–318. doi:10.1007/s00024-012-0525-1
- Anbazhagan P, Kumar A, Sitharam TG (2013a) Ground motion prediction equation considering combined data set of recorded and simulated ground motions. *Soil Dyn Earthq Eng* 53:92–108
- Anbazhagan P, Smitha CV, Kumar A, Chandran D (2013b) Seismic hazard assessment of NPP site at Kalpakkam, Tamil Nadu, India. *Nucl Eng Des* 259:41–64
- Anbazhagan P, Smitha CV, Abhishek Kumar (2014) Representative seismic hazard map of Coimbatore, India. *Eng Geol* 171:81–95
- Anbazhagan P, Bajaj K, Moustafa SSR, Al-Arifi NSN (2015) Maximum magnitude estimation considering the regional rupture character. *J Seismol*. <http://link.springer.com/article/10.1007%2Fs10950-015-9488-x> (published online)
- Atkinson GM, Boore DM (2003) Empirical ground-motion relations for subduction-zone earthquakes and their applications to Cascadian and other regions. *Bull Seismol Soc Am* 93:1703–1717
- Atkinson GM, Boore DM (2006) Earthquake ground-motion prediction equations for eastern North America. *Bull Seismol Soc Am* 96:2181–2205
- Banghar AR (1991) Mechanism solution of Nepal–Bihar earthquake of August 20, 1988. *J Geol Soc India* 37:25–30
- Baruah S, Gogoi NK, Erteleva Q, Aptikaev F, Kayal JR (2009) Ground motion parameters of Shillong plateau: one of the most seismically active zones of Northeastern India. *Earthq Sci* 22:283–291
- Bhatia SC, Ravi MK, Gupta HK (1999) A probabilistic seismic hazard map of India and adjoining regions. *Ann Geofis* 42:1153–1164
- Bommer JJ, Scherbaum F, Bungum H, Cotton F, Sabetta F, Abrahamson NA (2005) On the use of logic trees for ground-motion prediction equations in seismic-hazard analysis. *Bull Seismol Soc Am* 95:377–389
- Bommer JJ, Douglas J, Scherbaum F, Cotton F, Bungum H, Fäh D (2010) On the selection of ground-motion prediction equations for seismic hazard analysis. *Seismol Res Lett* 81(5):783–793
- Boore DM, Atkinson GM (2008) Ground-Motion Prediction Equations for the average horizontal component of PGA, PGV and 5% damped PSA at spectral periods between 0.01 and 10.0 s. *Earthq Spectra* 24(1):99–138
- Bormann P, Liu R, Ren X, Gutdeutsch R, Kaiser D, Castellaro S (2007) Chinese national network magnitudes, their relation to NEIC magnitudes and recommendations for new IASPEI magnitude standard. *Bull Seismol Soc Am* 95:58–74
- Campbell KW (1997) Empirical near-source attenuation relationships for horizontal and vertical components of peak ground acceleration, peak ground velocity and pseudo-absolute acceleration response spectra. *Seismol Res Lett* 68(1):154–179
- Campbell KW, Bozorgnia Y (2006) Next generation attenuation relation (NGA) Empirical ground motion models: can they be used for Europe. In: Proceedings of first European conference on earthquake engineering and seismology, Geneva, Switzerland, paper no. 458
- Campbell KW, Bozorgnia Y (2008) NGA ground motion model for the geometric mean horizontal component of PGA, PGV, PGD and 5 % damped linear elastic response spectra for period ranging from 0.01 to 10 s. *Earthq Spectra* 24:139–171
- Castellaro S, Mulargia F, Kagan YY (2006) Regression problems for magnitudes. *Geophys J Int* 165:913–930
- Cornell CA (1968) Engineering seismic risk analysis. *Bull Seismol Soc Am* 58:1583–1606
- Cotton F, Scherbaum F, Bommer JJ, Bungum H (2006) Criteria for selecting and adjusting ground-motion models for specific target regions: application to Central Europe and rock sites. *J Seismol* 10:137–156
- Das S, Gupta ID, Gupta VK (2006) A probabilistic seismic hazard analysis of Northeast India. *Earthq Spectra* 22:1–27
- Dasgupta S, Mukhopadhyay M, Nandy DR (1987) Active transverse features in the central portion of the Himalaya. *Tectonophysics* 136(1987):255–264
- Dasgupta S, Sengupta P, Mondal A, Fukuoka M (1993) Mineral chemistry and reaction textures in metabasites from the Eastern Ghats belt, India and their implications. *Miner Mag* 57:113–120

- Davis SD, Frohlich C (1991) Single-link cluster analysis, synthetic earthquake catalogs and aftershock identification. *Geophys J Int* 104:289–306
- Delavaud E, Scherbaum F, Kuehn N, Allen T (2012) Testing the global applicability of ground-motion prediction equations for active shallow crustal regions. *Bull Seism Soc Am* 102(2):702–721
- Delavaud E, Scherbaum F, Kuehn N, Riggelsen C (2009) Information-theoretic selection of ground-motion prediction equations for seismic hazard analysis: an applicability study using Californian data. *Bull Seismol Soc Am* 99:3248–3263
- Dewey JF, Bird JM (1970) Mountain belts and the new global tectonics. *J Geophys Res* 75(14):2625–2647
- Douglas J (2010) Consistency of ground-motion predictions from the past four decades. *Bull Earthq Eng* 8:1515–1526
- Douglas J, Mohais R (2009) Comparing predicted and observed ground motions from subduction earthquakes in the Lesser Antilles. *J Seism* 13(4):577–587
- EERI committee on seismic risk (1984) Glossary of terms for probabilistic seismic risk and hazard analysis. *Earthq Spectra* 1:33–36
- Frankel A (1995) Mapping seismic hazard in the central eastern United States. *Seismol Res Lett* 66(4):8–21
- Gansser A (1964) Geological history of Himalayan. *Geology of the Himalayas*, Wiley, Switzerland, pp 235–245
- Gardner JK, Knopoff L (1974) Is the sequence of earthquakes in southern California, with aftershocks removed, poissonian? *Bull Seismol Soc Am* 64(5):1363–1367
- Grünthal G (1998) European macroseismic scale 1998. *Cahiers du Centre EuropéendeGéodynamiqueet de Séismologie*, vol 15, Luxembourg
- GSI (2000) Eastern Nepal Himalaya and Indo-Gangetic Plains of Bihar. In: Narula PL, Acharyya SK, Banerjee J (eds) *Seismotectonics Atlas of India and its environs*. Geological Survey of India, India, pp 26–27
- Gupta ID (2010) Response spectral attenuation relations for inslab earthquakes in Indo-Burmese subduction zone. *Soil Dyn Earthq Eng* 30:368–377
- Gutenberg B, Richter CF (1956) Earthquake magnitude, intensity, energy and acceleration. *Bull Seismol Soc Am* 46:105–145
- Hintersberger E, Scherbaum F, Hainzl S (2007) Update of likelihood-based ground motion model selection for seismic hazard analysis in western central Europe. *Bull EarthqEng* 5:1–16
- Idriss IM (2008) An NGA empirical model for estimating the horizontal spectral values generated by shallow crustal earthquakes. *Earthq Spectra* 16:363–372
- IS 1893 (2002) Indian standard criteria for earthquake resistant design of structures, part 1-general provisions and buildings. Bureau of Indian Standards, New Delhi
- Joshi GC, Sharma ML (2008) Uncertainties in the estimation of M_{max} . *J Earth Syst Sci* 117(S2):671–682
- Kaklamanos J, Baise LG (2011) Model validations and comparisons of the next generation attenuation of ground motions (NGA–West) project. *Bull Seism Soc Am* 101(1):160–175
- Kanno T, Narita A, Morikawa N, Fujiwara H, Fukushima Y (2006) A new attenuation relation for strong ground motion in Japan based on recorded data. *Bull Seismol Soc Am* 96:879–897
- Khattri KN (1987) Great earthquakes, seismicity gaps and potential for earthquakes along the Himalayan plate boundary. *Tectonophysics* 38:79–92
- Kijko A, Sellevoll MA (1989) Estimation of earthquake hazard parameters from incomplete data files. Part I, utilization of extreme and complete catalogues with different threshold magnitudes. *Bull Seismol Soc Am* 79:645–654
- Kolathayar S, Sitharam TG, Vipin KS (2012) Deterministic seismic hazard microzonation of India. *J Earth Syst Sci* 121:1351–1364
- Kumar S (2012) Seismicity in the NW Himalaya India: fractal dimension, b -value mapping and temporal variation for hazard evaluation. *Geosci Res* 3(1):83–87
- Kumar A, Anbazhagan P, Sitharam TG (2013) Seismic hazard analysis of Lucknow considering local and active seismic gaps. *Nat Hazards* 69:327–350. doi:10.1007/s11069-0.13-0712-0
- Lai CG, Menon A, Corigliano M, Ornthamarrath, Sanchez HL, Dodagoudar GR (2009) Probabilistic seismic hazard assessment and stochastic site response analysis at the archaeological site of Kancheepuram in southern India. Research Report EUCENTRE 2009/01, IUSS Press, Pavia, ISBN 978-88-6198-037-2:250
- Lin PS, Lee CH (2008) Ground-Motion Attenuation relationship for subduction-zone earthquakes in Northeastern Taiwan. *Bull Seismol Soc Am* 98(1):220–240
- Mahajan AK, Thakur VC, Sharma ML, Chauhan M (2010) Probabilistic seismic hazard map of NW Himalaya and its adjoining area, India. *Nat Hazards* 53:443–457
- Malhotra PK (2006) Smooth spectra of horizontal and vertical ground motions. *Bull Seismol Soc Am* 96(2):506–518

- Mohindra R, Parkash B, Prasad J (1992) Historical geomorphology and pedology of the Gandak Megafan, Middle Gangetic Plains, India. *Earth Surf Process Land* 17:643–662
- Molchan G, Dmitrieva O (1992) Aftershock identification: methods and new approaches. *Geophys J Int* 109:501–516
- Nath SK, Thingbaijam KKS (2011) Peak ground motion predictions in India: an appraisal for rock sites. *J Seismol* 15:295–315
- Nath SK, Thingbaijam KKS (2012) Probabilistic seismic hazard assessment of India. *Seismol Res Lett* 83:135–149
- Nath SK, Vyas M, Pal I, Sengupta P (2005) A hazard scenario in the Sikkim Himalaya from seismotectonics spectral amplification source parameterization and spectral attenuation laws using strong motion seismometry. *J Geophys Res* 110:1–24
- Nath SK, Raj A, Thingbaijam KKS (2009) Kumar A (2009) Ground motion synthesis and seismic scenario in Guwahati city, a stochastic approach. *Seismol Res Lett* 80(2):233–242
- NDMA (2010) Development of probabilistic seismic hazard map of India. Technical report by National Disaster Management Authority, Government of India, New Delhi
- Parvez IA, Vaccari F, Panza GF (2003) A deterministic seismic hazard map of India and adjacent areas. *Geophys J Int* 155:489–508
- Reasenber P (1985) Second-order moment of central California seismicity 1969–1982. *J Geophys Res* 90:5479–5495
- Sabetta F, Lucantoni A, Bungum H, Bommer JJ (2005) Sensitivity of PSHA results to ground motion prediction relations and logic-tree weights. *Soil Dyn Earthq Eng* 25:317–329
- Savage WU (1972) Microearthquake clustering near Fairview Peak, Nevada, and in the Nevada seismic zone. *J Geophys Res* 77(35):7049–7056
- Scherbaum F, Cotton F, Smit P (2004) On the use of response spectral reference data for the selection and ranking of ground-motion models for seismic hazard analysis in regions of moderate seismicity: the case of rock motion. *Bull Seismol Soc Am* 94:1–22
- Scherbaum F, Bommer JJ, Bungum H, Cotton F, Abrahamson NA (2005) Composite ground-motion models and logic trees: methodology, sensitivities, and uncertainties. *Bull Seismol Soc Am* 95:1575–1593
- Scherbaum F, Delavaud E, Riggelsen C (2009) Model selection in seismic hazard analysis: an information theoretic perspective. *Bull Seismol Soc Am* 99:3234–3247
- Scordilis EM (2006) Empirical global relations converting MS and mb to moment magnitude. *J Seismol* 10:225–236
- SEISAT (2000) Seismotectonic Atlas of India and its environs. Geological Survey of India, India
- Sharma ML (1998) Attenuation relationship for estimation of peak ground horizontal acceleration using data from strong motions arrays in India. *Bull Seismol Soc Am* 88:1063–1069
- Sharma ML, Bungum H (2006) New strong ground motion spectral acceleration relation for the Himalayan region. In *First European conference on earthquake engineering and seismology*, p 1459
- Sharma ML, Douglas J, Bungum H, Kotadia J (2009) Ground-motion prediction equations based on data from Himalayan and Zagros regions. *J Earthq Eng* 13:1191–1210
- Singh RP, Aman A, Prasad YJJ (1996) Attenuation relations for strong ground motion in the Himalayan region. *Pure appl Geophys* 147:161–180
- Sinha R, Tandon SK, Gibling MR, Bhattacharjee PS, Dasgupta AS (2005) Late quaternary geology and alluvial stratigraphy of the Ganga basin. *Himal Geol* 26(1):223–340
- Spudich P, Joyner WB, Lindh AG, Boore DM, Margaris BM, Fletcher JB (1999) SEA99: a revised ground motion prediction relation for use in Extensional tectonic regions. *Bull Seism Soc Am* 89(5):1156–1170
- Sreevalsa K, Sitharam TG, Vipin KS (2011) Spatial variation of seismicity parameters across India and adjoining area. *Nat Hazards*. doi:10.1007/s11069-011-9898-1
- Stapp JC (1972) Analysis of completeness of the earthquake sample in the Puget Sound area and its effect on statistical estimates of earthquake hazard. *Proceeding of the International conference on microzonation*, vol 2. Seattle, USA, pp 897–910
- Stiphout VT, Zhuang J, Marsan D (2010) Seismicity declustering, community online resource for statistical seismicity analysis. <http://www.corssa.org>. Accessed 14 Jan 2014
- Strasser FO, Abrahamson NA, Bommer JJ (2009) Sigma: issues, insights, and challenges. *Seismol Res Lett* 80(1):40–56
- Stromeyer D, Grunthal G, Wahlstrom R (2004) Chi square regression for seismic strength parameter relations, and their uncertainty with application to an M_w based earthquake catalogue for central, northern and north-western Europe. *J Seismol* 8:143–153
- Takahashi T, Saiki T, Okada H, Irikura K, Zhao JX, Zhang J, Thoi HK, Somerville PG, Fukushima Y, Fukushima Y (2004) Attenuation models for response spectra derived from Japanese strong-motion

- records accounting for tectonic source types. 13th world conference of earthquake engineering, Vancouver, B.C., Canada, paper 1271
- Thingbaijam KKS, Nath SK, Yadav A, Raj A, Walling MY, Mohanty WK (2008) Recent seismicity in Northeast India and its adjoining region. *J Seismol* 12:107–123
- Uhrhammer RA (1986) Characteristics of northern and central California seismicity. *Earthq Notes* 1:21
- Valdiya KS (1976) Himalayan transverse faults and their parallelism with subsurface structures of north Indian plains. *Tectonophysics* 32:352–386
- Wallace K, Bilham R, Blume F, Gaur VK, Gahalaut V (2006) Geodetic constraints on the Bhuj 2001 earthquake and surface deformation in the Kachchh Rift basin. *Geophys Res Lett* 33:L10301. doi:10.1029/2006GL025775
- Wells DL, Coppersmith KJ (1994) New empirical relationships among magnitude, rupture length, rupture width, rupture area, and surface displacement. *Bull Seismol Soc Am* 4(84):975–1002
- Wiemer S, Wyss M (1994) Seismic quiescence before the landers ($M = 7.5$) and big bear ($M = 6.5$) 1992 earthquakes. *Bull Seismol Soc Am* 84:900–916
- Wiemer S, Wyss M (1997) Mapping the frequency-magnitude distribution in asperities: an improved technique to calculate recurrence times? *J Geophys Res* 102:15115–15128
- Woessner J, Stefan W (2005) Assessing the quality of earthquake catalogues: estimating the magnitude of completeness and its uncertainty. *Bull Seism Soc Am* 95(2):684–698
- Youngs RR, Chiou SJ, Silva WJ, Humphrey JR (1997) Strong ground motion relationship for subduction earthquakes. *Seismol Res Lett* 68:58–73
- Zhao JX, Zhang J, Asano A, Ohno Y, Oouchi T, Takahashi T, Ogawa H, Irikura K, Thio HK, Somerville PG, Fukushima Y, Fukushima Y (2006) Attenuation relations of strong ground motion in Japan using site classification based on predominant period. *Bull Seismol Soc Am* 96:898–913